

Spectral distortion anisotropies from single-field inflation

Giovanni Cabass,^a Enrico Pajer,^b and Drian van der Woude^b

^a Max-Planck-Institut für Astrophysik, Karl-Schwarzschild-Str. 1, 85741 Garching, Germany

^b Institute for Theoretical Physics and Center for Extreme Matter and Emergent Phenomena,
Utrecht University, Princetonplein 5, 3584 CC Utrecht, The Netherlands

Abstract

Distortions of the Cosmic Microwave Background energy spectrum of the μ type are sensitive to the primordial power spectrum through the dissipation of curvature perturbations on scales $k \simeq 50 - 10^4 \text{ Mpc}^{-1}$. Their angular correlation with large-scale temperature anisotropies is then sensitive to the squeezed limit of the primordial bispectrum. For inflationary models obeying the single-field consistency relation, we show that the observed μT angular correlation that would correspond to the local shape vanishes exactly. All leading non-primordial contributions, including all non-linear production and projection effects, are of the “equilateral shape”, namely suppressed by k^2/\mathcal{H}_f^2 , where $\mathcal{H}_f \simeq 10^{-1} \text{ Mpc}^{-1}$ is the Hubble radius at the end of the μ -era. Therefore, these non-primordial contributions are orthogonal to a potential local primordial signal (*e.g.* from multi-field inflation). Moreover, they are very small in amplitude. Our results strengthen the position of μ distortions as the ultimate probe of local primordial non-Gaussianity.

Contents

1	Introduction and main results	2
2	General strategy and assumptions	4
2.1	Preliminaries	4
2.2	General strategy	5
2.3	Assumptions	6
3	Generation of μ-type spectral distortion	7
3.1	A master equation for the production of μ distortion	7
3.2	μ production at quadratic order	9
3.3	μ production at cubic order	10
4	Evolution of μ-type spectral distortion	11
4.1	From CFC to global coordinates	11
4.2	Non-linear evolution	12
4.3	First order in the gradient of the long mode and beyond	13
5	Observed μT cross-correlation	14
5.1	Contributions to the observed $\langle \mu T \rangle$	14
5.2	μT angular correlation and Fisher forecast	17
6	Discussion and conclusions	19
A	Window function for μ from super-Hubble scales	20
B	From the μ-era to recombination	22
B.1	Leading order	24
B.2	Subleading orders	25
C	Cancellation of $f_{\text{NL}} = 1 - n_s$ in global coordinates	25
D	Average μ distortions in the sky	26
E	Moments of the Boltzmann equation	27
F	Details of the Fisher forecast	28
G	Fisher forecast for a PIXIE-like experiment	29

1 Introduction and main results

As it is well-known [1], μ -type distortions of the Cosmic Microwave Background (CMB) energy spectrum probe primordial perturbations on scales $k \simeq 50 - 10^4 \text{ Mpc}^{-1}$ through the dissipation of acoustic waves in the photon-electron-baryon fluid (for a recent review see [2] and references therein). In presence of primordial non-Gaussianity, the amplitude of the dissipation becomes spatially dependent on large scales and it gives rise to an angular correlation $C_\ell^{\mu T}$ between $\mu(\hat{\mathbf{n}})$ and large-scale $T(\hat{\mathbf{n}})$ anisotropies, which are sourced by the same large-scale modes that modulate the dissipation [3]. Indeed, with local non-Gaussianity we expect an angular cross-correlation between temperature anisotropies and fractional μ anisotropies given by $-12f_{\text{NL}}C_\ell^{TT}$ [3,4].¹ Much recent work has been devoted to better understand and model this mechanism as well as forecasting and measuring the constraining power of $C_\ell^{\mu T}$ for primordial non-Gaussianity [4,8–19].

As for CMB temperature anisotropies, one expects late-time evolution to “contaminate” any contribution from primordial non-Gaussianity. For example, even for single-field inflation satisfying the Maldacena’s consistency relation there is a non-primordial contribution to the squeezed CMB bispectrum of the local shape, $B_{\ell_L \ell_S \ell_S}^{TTT} \sim C_{\ell_L}^{TT} C_{\ell_S}^{TT}$ [20–27]. For $\ell_L \lesssim 100$, the long mode is outside the Hubble radius at recombination and therefore it cannot change the local physics to leading and subleading order in derivatives. Instead, the long mode affects photons as they travel from the last-scattering surface to the observer. For single-field inflation models that satisfy the consistency relation, this effect is all the result [23,27,28].

In this paper, we show that an analogous *non-primordial contamination is instead absent for the $C_\ell^{\mu T}$ angular spectrum: in single-field attractor inflation $C_\ell^{\mu T}$ vanishes up to corrections of order k^2/\mathcal{H}_f^2* , where $k \sim \ell/\eta_0$ is the long-wavelength temperature mode and $\mathcal{H}_f \simeq 10^{-1} \text{ Mpc}^{-1}$ is the Hubble radius at the end of the so-called μ -era, $z \simeq 5 \times 10^4$, when μ distortions stop being generated. Non-primordial contributions to μT arise from non-linear “production” effects, *i.e.* non-linearities during the μ -era, and from non-linear “propagation” effects, *i.e.* non-linearities in the evolution from the μ -era to observation. We show that the leading non-primordial contributions lead to a $C_\ell^{\mu T}$ that has the same ℓ -dependence as equilateral non-Gaussianity, as opposed to local non-Gaussianity. In addition, the amplitude of these contributions is very small and would be detectable only by a very futuristic almost cosmic variance-limited experiment (see Section 5.2 for details).

Our results can be intuitively understood as follows. To compute $C_\ell^{\mu T}$, we can divide the sky in patches, measure the average chemical potential $\mu(\hat{\mathbf{n}})$ in each patch, and then see if it correlates with $T(\hat{\mathbf{n}})$. All modes that are observationally relevant were super-Hubble during the μ -era, and therefore their effect on the production of μ (which is a local observable) were suppressed by at least two derivatives over the Hubble radius. Therefore, these non-primordial production effects lead to an effective equilateral shape of $C_\ell^{\mu T}$, as opposed to local.² No spatial variation of μ can come from the initial conditions either, if the consistency relation of single-clock inflation is satisfied [27]. We see, then, that there are only two effects that could contribute to $C_\ell^{\mu T}$, both coming from so-called “projection effects” as the photons travel to us:

¹We will consider only local f_{NL} in this work. Conventionally, it is defined in terms of the Newtonian potential during matter domination, *i.e.* $B_\Phi(k_1, k_2, k_3) = -2f_{\text{NL}}P_\Phi(k_1)P_\Phi(k_2) + 2$ perms., where $\zeta = -\frac{5\Phi}{3}$ [5,6]. Notice also that we use the notation of [7] for the comoving curvature perturbation.

²We use the loose language of “equilateral shape” and “local shape” to refer to the ℓ dependence of $C_\ell^{\mu T}$ that would be generated by equilateral or local primordial non-Gaussianity.

- The same physical length scale appears at different angular sizes to the observer, due to the expansion and distortion of the photon geodesics caused by a long mode.
- Photons experience a different redshift in different directions due to the presence of a long mode.

The modulation of physical scales does not lead to any effect when we compute $C_\ell^{\mu T}$ because the average μ in a patch of the sky does not possess any intrinsic length scale. Let us contrast this with the temperature bispectrum. There, what we are doing is measure the TT angular power spectrum in each patch and check if it correlates with a long temperature mode. In this case, we do have a physical length scale that can be distorted by the long mode, namely to the distance between the peaks of the short-scale temperature power spectrum. When we consider the μT power spectrum, instead, we are just looking at the average μ in a patch, so there is no “ruler” whose length the long mode can perturb. In other words, a homogeneous $\mu(\mathbf{x}) = \mu$ remains such under evolution after the μ -era because only inhomogeneities in $\mu(\mathbf{x})$ can be lensed or deformed. The second effect also vanishes for $C_\ell^{\mu T}$. To see this, let us contrast it again with the temperature bispectrum. In that case, a long mode modifies the Sachs-Wolfe + Doppler + Integrated Sachs-Wolfe formula relating inhomogeneities in the photon distribution at recombination to temperature anisotropies at the observer’s point, and changes the average temperature in each patch (temperature with respect to which the anisotropies are defined). Instead, since μ does not depend on the photon energy, we can and do always define it to be the dimensionless quantity $\mu = -\mu_{\text{th}}/T$, where μ_{th} has its usual definition from thermodynamics. This variable does not redshift: the evolution after the μ -era leaves it unchanged.

Finally, in addition to showing that the non-primordial contributions to μT cross-correlations are of all of the equilateral shape and small in amplitude, we also derive two new, albeit more technical, results:

- We rewrite the hydrodynamic description of [9] in a manifestly covariant formalism. This allows us to write simple non-perturbative expressions for the generation of μ distortions, such as Eq. (3.6).
- We derive for the first time a Fourier window function for the generation of μ distortions at second order in perturbations that is valid for modes of all wavelengths. This is to be contrasted with the expressions used in the literature that are valid only in the sub-Hubble regime. Although the dissipation does indeed mostly come from sub-Hubble modes, our general-relativistic formula is nevertheless essential to correctly compute one of the contributions to the $\langle \mu T \rangle$ correlator beyond the result discussed above, and prove that it is subleading with respect to it.

Outline The outline of the paper is as follows. In Section 2 we describe the general strategy of the computation and review our assumptions. In Section 3 we review the creation of μ distortions from Silk damping, *i.e.* by viscosity, and estimate the effect of the long-wavelength temperature mode on μ production. In Section 4 we discuss the evolution of μ from the end of the μ -era to the observer following the approach of [23], and show that no correlation with the long mode is generated during this time. In Section 5, then, we compute the leading non-primordial effect on the observed μT correlator, which comes from the modulation of the μ production from Silk damping by the long-wavelength temperature mode. In this Section we also discuss other subleading contributions, *i.e.* the effect of temperature non-linearities and

of heat conduction. Finally we show that these non-primordial contributions are orthogonal to those of a local f_{NL} . Conclusions are drawn in Section 6. The Appendices from A to F contain some technical details on the computations of Sections 3, 4, and 5. The Appendix G confirms that also for a PIXIE-like experiment the impact of the non-primordial contributions on $\sigma(f_{\text{NL}})$ will be negligible.

2 General strategy and assumptions

In this section, we outline our general strategy for the calculation of the μT cross-correlation in single-field inflation. Then, for the convenience of the reader, we summarize and discuss the main assumptions and approximations we will employ.

2.1 Preliminaries

Our goal is to compute the largest contribution to the observable μT cross-correlation at late times. For multi-field models with sizable *local* primordial non-Gaussianity, $f_{\text{NL}} \gg \mathcal{O}(n_s - 1)$, the largest contribution is proportional to f_{NL} and was first computed in [3]. Instead, as anticipated in [3], for single-field inflation the well-known contribution $f_{\text{NL}} = (1 - n_s)$ is a gauge artifact and should cancel exactly in the final observable result. Here, besides showing this more explicitly, we establish that *the next largest surviving contribution to $\langle \mu T \rangle$ is the non-linear evolution of short modes during the μ -era, which feel a long mode as a local spatial curvature*. The double derivative suppression of this non-linear effect leads to a final contribution to μT that is of the equilateral shape and small in amplitude.

Let us introduce and define some quantities of interest. We expand the perturbations in μ and T as

$$\mu = \mu^{(1)} + \mu^{(2)} + \mu^{(3)} + \dots, \quad (2.1a)$$

$$T = T^{(1)} + T^{(2)} + \dots. \quad (2.1b)$$

Note that μ contains a linear contribution $\mu^{(1)} \sim \mathcal{O}(\zeta)$ due to heat conduction [9]. An additional linear contribution comes from perturbations to adiabatic cooling. This contribution is suppressed by the baryon-to-photon number ratio and turns out to be negligible. This is further discussed in Section 2.3, around Eq. (2.6). Besides, as argued in [9], bulk viscosity effects are suppressed by the photon-to-baryon ratio squared and can be neglected. Then, the standard and largest contribution to $\langle \mu \rangle$ starts at quadratic order, $\mu \sim \mathcal{O}(\zeta^2)$. Also, we used the fact that we want to compute $\langle \mu T \rangle$ up to $\mathcal{O}(\zeta^4) \sim \mathcal{O}(\Delta_\zeta^4)$,³ with $\Delta_\zeta^2 \simeq 2 \times 10^{-9}$ being the amplitude of primordial perturbations (on CMB scales). Expanding in perturbations one finds

$$\langle \mu T \rangle = \langle \mu^{(2)} T^{(1)} \rangle_{\text{NG}} + \langle \mu^{(1)} T^{(1)} \rangle_{\text{G}} + \langle \mu^{(3)} T^{(1)} \rangle_{\text{G}} + \langle \mu^{(2)} T^{(2)} \rangle_{\text{G}} + \dots, \quad (2.2)$$

where the label ‘‘NG’’ reminds us that $\langle \mu^{(2)} T^{(1)} \rangle$ is proportional to the primordial bispectrum, while the other terms are not. Expressions for $T^{(1)}$, $T^{(2)}$ are known in the literature while $\mu^{(2)}$, $\mu^{(3)}$ are not fully known and so we need to compute them here:

- A sub-Hubble approximation for $\mu^{(2)}$ has been derived and used many times in the literature (most recently for example in [16]). However, this sub-Hubble approximation is

³The term $\langle \mu^{(1)} T^{(3)} \rangle$ is suppressed by Δ_ζ^2 with respect to $\langle \mu^{(1)} T^{(1)} \rangle$ and is therefore negligible.

not sufficient for calculating the $\langle \mu^{(2)} T^{(2)} \rangle$ correlator on observationally relevant scales,⁴ so in Section 3 we derive a fully general-relativistic expression for $\mu^{(2)}$ that is valid at any scale, sub- and super-Hubble.

- The next-to-leading order contribution $\mu^{(3)}$ is not yet known. Here we estimate its leading term, for the purpose of computing $\langle \mu^{(3)} T^{(1)} \rangle$ on observationally relevant scales.

The calculation of $\mu^{(3)}$ is the most technically challenging part of our work and will be presented in Sections 3 and 4. To guide the reader, let us outline our general strategy.

2.2 General strategy

First of all, let us separate the evolution *during* the μ -era, *i.e.* the period of time when μ can be created, from the evolution *after* the μ -era until now, when only an existing μ can be lensed or dissipated. These are discussed in Section 3 and Section 4, respectively. We will prove that the only relevant non-linearities arise during the μ -era.

Since μ starts at $\mathcal{O}(\zeta^2)$, computing $\mu^{(3)}$ requires the knowledge of ζ at second order, and in particular of the long-short mode coupling $\zeta^{(2)} \sim \zeta_S^{(1)} \zeta_L^{(1)}$. This mode coupling is generated only when the short modes are inside the Hubble radius,⁵ either during inflation or after Hubble re-entry during the μ -era. The non-linearities during the inflationary and μ -era can each be computed either in global coordinates or in local physical coordinates, a.k.a. Conformal Fermi Coordinates (CFC) [29, 30]. The CFC calculation at zeroth and first order in k_L gives a vanishing long-short mode coupling both during inflation and the μ -era by construction. At $\mathcal{O}(k_L^2)$ the inflationary period leads to slow-roll suppressed terms [31]

$$\zeta^{(2)} \supset 0.1 \times (n_s - 1) \left(\frac{k_L}{k_S} \right)^2 \zeta_L^{(1)} \zeta_S^{(1)} \quad (\text{inflation, CFC}) . \quad (2.3)$$

At the same order $\mathcal{O}(k_L^2)$, the μ -era induces non-linearities of order

$$\zeta^{(2)} \supset \left(\frac{k_L}{\mathcal{H}} \right)^2 \zeta_L^{(1)} \zeta_S^{(1)} \quad (\mu\text{-era, CFC}) . \quad (2.4)$$

These can be understood as resulting from the evolution of short modes in the background of the long mode, which mimics a spatial curvature in the isotropic case. In Section 5.1, we argue that \mathcal{H} should be the Hubble scale at the end of the μ -era. Since it is mostly the dissipation of sub-Hubble modes that sources μ , in the above formulae $k_S \gg \mathcal{H}$ and the non-linearities in the μ -era are much larger than those during inflation, which can safely be neglected.

Up to this point, we have been able to neglect the constant and gradient part of the long ζ mode by construction. This works as long as the long mode is super-Hubble. However, we wish to compute the evolution of the $\langle \mu T \rangle$ all the way up to today, including the effect of modes that were super-Hubble at the time of μ production, but are sub-Hubble now. The inclusion of these “projection effects” proceeds in two steps.

First we have to include the constant and gradient long modes in our computation. As long as they are super-Hubble, this can be done at any preferred moment by Weinberg’s

⁴The sub-Hubble approximation is instead sufficient to compute $\langle \mu^{(2)} \mu^{(2)} \rangle$ because the incorrect k scaling, when squared, makes the integral still correctly peak on sub-Hubble scales, where the window function is a good approximation of the exact result.

⁵When the short modes are super-Hubble, they freeze out and no sizeable non-linearity is generated.

adiabatic mode construction [22,23,28,32]: the effect of the long modes on CFC computations is equivalent to a change of coordinates. For us, the most convenient time to include these modes is at the end of the μ -era. In fact, as we show in Section 4, since the expectation value of μ at this time is both independent of space and time, the effect of the coordinate change is zero!

Subsequently, we need to evolve the distribution of photons from the end of the μ -era to today. Once again, we prove that the expectation value of μ is untouched during the evolution. The intuition is that any physical effect, such as lensing or dissipation, does not affect a homogeneous μ . Hence, no spatial variation of μ can be generated if there is none to begin with. In conclusion, no contribution to the μT cross-correlation arises from the non-linear evolution after the μ -era.

Note that Maldacena's $(n_s - 1)$ from the derivative of the short scale power spectrum [7] appears nowhere in this computation. This is a consequence of our convenient choice of the time at which we change from local (CFC) to global coordinates. If one were to insist on using global coordinates at some earlier stage, $(n_s - 1)$ would appear. In that case, however, one would have to compute μ production in global coordinates and for consistency this should to be done at cubic order $\mu^{(3)} = \mathcal{O}(\zeta^3)$. This is further discussed in Appendix C. Since the final prediction for $\langle \mu T \rangle$ is independent of the method we use to calculate it, we stick to the most straightforward strategy.

2.3 Assumptions

Let us summarize and discuss the main approximations and assumptions in our analysis.

Hydrodynamic approximation The full calculation of the CMB spectrum anisotropies at second order in perturbations would require solving the inhomogeneous collisional Boltzmann equation, which is undoubtedly a daunting task. On the other hand, the system is perturbative and well amenable to the use of effective theory techniques, such as the hydrodynamical approach developed in [9]. Here we follow this analytical approach, which makes the physics transparent at the cost of a tiny error coming from the approximation of thermodynamical equilibrium. The only shortcoming of this approach is that the boundaries of the μ and y eras must be given as an added input, derived from the homogeneous solution of the Boltzmann equation. Using for example some simple analytic fits to detailed numerical simulations (see *e.g.* [33]) one expects this to lead to a mistake at the percent level.

Single fluid approximation In principle, one should keep track of five fluids: photons, Dark Matter, neutrinos, baryons and electrons. Neutrinos are still relativistic at the time of interest and free streaming. Therefore neutrinos inhomogeneities quickly decay on sub-Hubble scales. We approximate the neutrinos as a homogeneous fluid, which contributes only to the background evolution. Dark Matter on sub-Hubble scales has inhomogeneities that grow very little (logarithmically) during radiation domination and linearly in $a(t)$ during matter domination. During the μ -era, the energy density of Dark Matter is much smaller than that of the photons, $\rho_{\text{DM}}/\rho_\gamma < 0.1$. Since the interaction with any other component is gravitational, Dark Matter inhomogeneities can also be neglected during the μ -era. Instead, we keep all Dark Matter inhomogeneities at later times, after the μ -era, since they could be important for example for the lensing calculation. Baryons, electrons and photons are tightly coupled before recombination and so the respective fluid velocities are the same to a good approximation. We can therefore treat them as a single fluid with some common velocity U^μ

and with

$$\rho = \rho_\gamma + \rho_b \simeq \rho_\gamma + m_p n_b , \quad (2.5a)$$

$$p = p_\gamma + p_b \simeq p_\gamma , \quad (2.5b)$$

where the labels γ and b refer to photons and baryons respectively and m_p is the proton mass. Here we neglected the small contribution due to electrons, $m_e/m_p \simeq 5 \times 10^{-4}$, and neglected the effect of baryon temperature, which are suppressed by the baryon-to-photon number ratio $r = n_b/n_\gamma \simeq 5 \times 10^{-10}$.

Adiabatic cooling Even for an ideal fluid, there is some homogeneous μ production during the μ -era due to adiabatic cooling, which is proportional to the photon-to-baryon number ratio r . This is estimated to be $\bar{\mu}_{AC} \simeq -2.7 \times 10^{-9}$ for the *Planck* 2015 best-fit parameters (see *e.g.* [34, 35] and references therein) and therefore slightly smaller than the homogeneous contribution from Silk damping, $\langle \mu_S \rangle \simeq 2 \times 10^{-8}$.

One might worry that long modes also modulate $\bar{\mu}_{AC}$, which then contributes to $\langle \mu T \rangle$. Fortunately, the treatment of the effect of long modes on $\bar{\mu}_{AC}$ is analogous to the treatment of μ from Silk damping. During the μ -era, the non-linearities are computed in CFC, meaning corrections are at most of the form

$$\mu_{AC}^{(1)} \supset \left(\frac{k_L}{\mathcal{H}} \right)^2 \bar{\mu}_{AC} \zeta_L^{(1)} \quad (\mu\text{-era, CFC}) . \quad (2.6)$$

After the μ -era, we compute the change to global coordinates and the subsequent evolution in exactly the same way, and since $\bar{\mu}_{AC}$ is also homogeneous and frozen, it is untouched throughout its evolution and no further correlation with the long modes is induced. If indeed $\bar{\mu}_{AC} \ll \langle \mu_S \rangle$ as suggested by current data, we expect Eq. (2.6) to lead to an effect that is subdominant with respect to the term $\langle \mu^{(3)} T^{(1)} \rangle_G$ in Eq. (2.2) (which is discussed in Section 3.3 below).

3 Generation of μ -type spectral distortion

In this section, we review the generation of μ -type spectral distortion to leading (second) order in perturbations, following [9]. The formulae in the literature (see *e.g.* [1, 3, 16, 18]) for μ from the dissipation of acoustic modes are valid only in the sub-Hubble regime, which is indeed where most of the effect comes from. Here, we derive a more general formula for μ that is instead valid for arbitrary long wavelength perturbations. Our main result, Eqs. (3.7) and (3.8), can be thought of as the general-relativistic extension of the Fourier space window function used in the literature. This general-relativistic window function is essential for the correct calculation of the μT cross-correlation in Section 5. A series of technical details are collected in Appendix A.

3.1 A master equation for the production of μ distortion

Following our assumptions, we model the electron-photon-baryon plasma as a single, viscous fluid with four velocity U^μ and temperature $T(x)$. After $z_i \simeq 2 \times 10^6$, all processes that change photon number become inefficient and the number of photons n leads to a covariantly conserved local current $\nabla_\mu N^\mu = 0$.⁶ This conserved quantity is the statistical conjugate of the

⁶We omit the label γ for the photon number current because this is the only current we will be interested in.

dimensionless chemical potential $\mu(x)$. Kinetic equilibrium ceases to be a good approximation when Compton scattering becomes inefficient at redistributing momentum, around $z = z_f \simeq 5 \times 10^4$. After $z = z_f$, the released energy goes into different kinds of distortions (the so-called r distortions and y distortions: we refer to [36–38] and references therein for details). The transitions around z_i and z_f are actually smooth and can be captured quantitatively using the Green's functions fits of [33]. In the following, we derive a formula for the evolution of μ during this period.

Viscous corrections lead to the dissipation of acoustic waves in the plasma and generate entropy. Such entropy increase cannot be balanced by a change in the number of photons, so the average energy and entropy per photon grow. Working at linear order in μ , we can relate the chemical potential to the specific entropy (the entropy per particle), namely the ratio between the rest-frame entropy density s and number density of photons n :

$$\frac{s}{n} = \frac{2\pi^4}{45\zeta(3)} [1 + (A_n - A_s)\mu] , \quad (3.1)$$

where we define $A_s \equiv \frac{135\zeta(3)}{2\pi^4}$, $A_n \equiv \frac{\pi^2}{6\zeta(3)}$ following [9]. This equation tells us that we can compute the evolution of μ if we know how s and n evolve. For a perfect fluid, we know that the ratio s/n will be constant along the fluid lines (n is conserved during the μ -era). In presence of viscous corrections, however, the conservation of entropy and photon number density take the form [9, 39, 40]⁷

$$\nabla_\mu(nU^\mu + \Delta N^\mu) = 0 , \quad (3.2a)$$

$$\nabla_\nu(sU^\nu + \mu\Delta N^\nu) = -\frac{\Delta T^{\mu\nu}\nabla_\nu U_\mu}{T} + \Delta N^\nu\nabla_\nu\mu , \quad (3.2b)$$

where ΔN^μ and $\Delta T^{\mu\nu}$ are the leading (in an expansion in $t_\gamma \times \partial_\mu$, with $t_\gamma = (\sigma_T n_e)^{-1}$ being the photon mean free path) viscous corrections to the photon number density current and the stress-energy tensor. In accordance with our approximations, discussed in Section 2, in writing Eqs. (3.2) we have neglected the contribution of baryon (and electron) conservertion to the total entropy, which is indeed suppressed by the baryon-to-photon number ratio r . Using Eqs. (3.2), we arrive at

$$\begin{aligned} U^\mu\nabla_\mu\left(\frac{s}{n}\right) &= -\frac{\mu}{n}\nabla_\nu\Delta N^\nu - \frac{\Delta T^{\mu\nu}\nabla_\nu U_\mu}{nT} + \frac{s}{n^2}\nabla_\mu\Delta N^\mu \\ &= -\frac{\Delta T^{\mu\nu}\nabla_\nu U_\mu}{nT} + \frac{\pi^6}{45\zeta(3)^2 T^3}\nabla_\mu\Delta N^\mu + \mathcal{O}(\mu^2) , \end{aligned} \quad (3.3)$$

where we used the fact that $\Delta N^\mu = \mathcal{O}(\mu)$ and stopped at linear order in μ . Indeed, as shown in [9, 39, 40], ΔN^μ and $\Delta T^{\mu\nu}$ take the form

$$\Delta N_\nu = -\chi\left(\frac{nT}{\rho + p}\right)^2 P_\nu^\rho\nabla_\rho\mu , \quad (3.4a)$$

$$\Delta T_{\mu\nu} = -2\eta P_{(\mu}^\rho\nabla_\rho U_{\nu)} + \left(\frac{2\eta}{3} - \zeta\right)\nabla_\rho U^\rho P_{\mu\nu} , \quad (3.4b)$$

⁷The original derivation in [39] used the convention in which U^μ is the velocity of particle transport, in which case $\Delta N^\mu = 0$. Instead, in [9, 40] the velocity refers to the transport of energy, defined by the condition $U^\mu\Delta T_{\mu\nu} = 0$. In this case $\Delta N^\mu \neq 0$. We use here the latter convention.

where the coefficients χ , η and ζ are, respectively, the heat conduction, shear viscosity and bulk viscosity, and $P^\mu_\nu \equiv \delta^\mu_\nu + U^\mu U_\nu$ is the projector on the instantaneous rest frame of the fluid. As shown in [9], ΔN^μ vanishes up to terms of order of the baryon loading, defined as $R \equiv 3\rho_b/(4\rho_\gamma)$. Additionally, the bulk viscosity is also suppressed by $r^2 \simeq 10^{-19}$ with respect to the shear viscosity. For this reason, ζ can be safely neglected in the following [9]. For the moment, we drop also the heat conduction χ : its effect will be discussed in more detail in Section 5.1. Therefore, with only the shear viscosity remaining, Eq. (3.3) becomes

$$U^\mu \nabla_\mu \left(\frac{s}{n} \right) = \frac{2\eta}{nT} \left(P^\rho_{(\mu} \nabla_\rho U_{\nu)} \nabla^\nu U^\mu - \frac{(\nabla_\mu U^\mu)^2}{3} \right), \quad (3.5)$$

where η is equal to $\frac{16}{45}t_\gamma\rho_\gamma$. Using the fact that $\nabla_\mu U_\nu = HP_{\mu\nu}$ on an FLRW background, it is straightforward to see that the right-hand side of the above equation starts at second order in perturbations. Moreover, Eq. (3.5) explicitly shows that μ can be generated only if viscous corrections are present: solving for μ perturbatively in $t_\gamma \times \partial_\mu$ and stopping at first order in this expansion allows us to evaluate the thermodynamical quantities in the pre-factor on the right-hand side at zeroth order in μ :

$$U^\nu \nabla_\nu \mu = \frac{8t_\gamma}{15(A_n - A_s)} \left(P^\rho_{(\mu} \nabla_\rho U_{\nu)} \nabla^\nu U^\mu - \frac{(\nabla_\mu U^\rho)^2}{3} \right). \quad (3.6)$$

This expression, which is valid in the hydrodynamical approximation⁸ to all orders in perturbations, can be thought of as a generalization of Eq. (1.7) in [9]. The generation of μ will proceed in time according to Eq. (3.6).

3.2 μ production at quadratic order

Eq. (3.6) can be solved at leading order in cosmological perturbation theory, to arrive at an expression for the generated μ distortion in terms of the primordial fluctuations. The final result is that $\mu = \mathcal{O}(\zeta^2)$ can be written in terms of window function W as (we use the shorthand $\int_{\mathbf{k}}$ to denote $\int \frac{d^3k}{(2\pi)^3}$)

$$\mu^{(2)}(\eta_f, \mathbf{x}) = \int_{\mathbf{k}_1} \int_{\mathbf{k}_2} \zeta(\mathbf{k}_1) \zeta(\mathbf{k}_2) W(\mathbf{k}_1, \mathbf{k}_2) e^{i(\mathbf{k}_1 + \mathbf{k}_2) \cdot \mathbf{x}}, \quad (3.7)$$

where the general-relativistic Fourier space window function⁹ (derived in Appendix A)

$$W(\mathbf{k}_1, \mathbf{k}_2) \equiv \frac{8}{15(A_s - A_n)} \left[(\mathbf{k}_1 \cdot \mathbf{k}_2)^2 - \frac{1}{3} k_1^2 k_2^2 \right] \times \int_0^\infty dz' \left(\frac{t_\gamma}{\mathcal{H}} \right) \frac{T_v(z', k_1) T_v(z', k_2)}{\mathcal{H}^2} \mathcal{J}_\mu(z'). \quad (3.8)$$

⁸In the perfect fluid limit, *i.e.* $t_\gamma = 0$, Eq. (3.6) tells us that μ is simply frozen along the fluid lines, *i.e.* $U^\rho \nabla_\rho \mu = 0$. To finite order in t_γ , the equation describes not only the generation of μ , but also the damping of μ inhomogeneities due to viscosity [9], during the μ -era. The damping and evolution of μ inhomogeneities after the μ -era will be discussed in Section 4 and Appendix B.

⁹Although most of the dissipation takes place on sub-Hubble scales, it is very important for us to use the fully relativistic W given above in our calculation. In fact, the sub-Hubble approximation, *e.g.* Eq. (6) in [3] has the wrong scaling as one of the two wavenumber goes to zero. Using this sub-Hubble approximation instead of W gives a very small corrections in the computation of $\langle \mu T \rangle$ from primordial non-Gaussianity. On the other hand, it is essential to use the full W when computing $\langle \mu^{(2)} T^{(2)} \rangle$, which is of one the second-order contributions to μT .

Here, T_v is the transfer function of the velocity potential and \mathcal{J}_μ is an analytic fit to the time window function computed numerically in [33]. Moreover, we recall that during radiation domination the damping scale and the photon mean free path $t_\gamma = (\sigma_T n_e)^{-1}$ are related by the approximate expression $k_D^{-1} \simeq \sqrt{t_\gamma \eta/a} = \sqrt{t_\gamma/a \mathcal{H}}$, *i.e.* $k_D^2 \simeq a \mathcal{H}/t_\gamma$ [41].

The window function of Eq. (3.8) agrees with, for instance, Eq. (1.7) in [9], even though that was derived for sub-Hubble scales only. Notice that when the angle between the momenta in this window function is zero (which happens for instance upon taking an ensemble average of μ itself), this window function also matches the window function in [16]: however, this reference *does not* write the full window function including super-Hubble modes, which is essential to this work. Moreover, we stress that the spatial structure in our formula differs from [16] for generic momenta. From Eq. (3.8) we also see how this window function has the expected behavior when either one of the two wavenumbers goes to zero, namely $W(k_1, k_2) \sim k_1^2$ for $k_1 \ll \mathcal{H}$, and similarly for k_2 . In addition, sub-Hubble modes much longer than the Silk damping scale during the μ -era, $\mathcal{H} \ll k_{1,2} \ll k_D$ are suppressed by $k_1 k_2 / k_D^2(z_f)$, where k_D at the end of the μ -era is roughly $k_D(z_f) \simeq 50 \text{ Mpc}^{-1}$.

3.3 μ production at cubic order

We now estimate the production of μ at cubic order, $\mu^{(3)}$, which in Section 5 we will find to give the leading contribution to the μT correlation in single-field inflation. One can write the dependence of the expectation value of μ_S on a long ζ mode as

$$\langle \mu_S \rangle_{\zeta_L}(\eta, \mathbf{x}) = \langle \mu_S \rangle_{\zeta_L=0} - \frac{b_1}{\Lambda^2} \partial^2 \zeta_L(\eta, \mathbf{x}) \langle \mu_S \rangle_{\zeta_L=0} + \text{higher derivatives} , \quad (3.9)$$

where $\partial^2 = \delta_{ij} \partial_i \partial_j$ and

$$\frac{b_1}{\Lambda^2} \equiv -\frac{1}{\langle \mu_S \rangle_{\zeta_L=0}} \left[\frac{\partial \langle \mu_S \rangle_{\zeta_L}}{\partial (\partial^2 \zeta_L)} \right]_{\zeta_L=0} . \quad (3.10)$$

Here we have in mind b_1 of order unity (the sign has been chosen for later convenience: more precisely, with this choice we will have a contribution $C_\ell^{\mu T} \sim b_1$ in Section 5.2). Notice that the physical situation here is the same as the one that leads to the bias expansion in the context of galaxy clustering (see [42] for a comprehensive review), *i.e.* that of a separation between the scale of local physics and the scale at which we measure correlation functions: for this reason, in the following we will refer to b_1 as the “bias” parameter.

The question now is: given that we want $b_1 \sim \mathcal{O}(1)$, what is the value of the scale Λ that suppresses $\partial^2 \zeta_L$? To answer this, first observe that spatial curvature of the local, “separate” universe is related to the second derivative of ζ as [30, 43]

$$\frac{\partial^2 \zeta}{\mathcal{H}^2} \sim \Omega_K . \quad (3.11)$$

Then, since spatial curvature modifies the evolution of the Hubble rate and the evolution of short scale modes at order unity, we expect the suppression scale Λ to be approximately the (comoving) Hubble scale at the end of the μ -era (where it is smallest), which we call \mathcal{H}_f . Alternatively, one could argue that at leading order in t_γ , there is no additional scale available besides Hubble. This is seen, for example, from the general-relativistic expression for the window function: if both modes are sub-Hubble, *i.e.* $\mathcal{H} \ll k_{1,2} \ll k_D$, the suppression is $k_1 k_2 / k_D^2$, manifestly showing that μ is created by damping. If both modes are super-Hubble, it becomes $k_1^2 k_2^2 / k_D^2 \mathcal{H}^2$. We here care about the third-order contribution, with at least one

super-Hubble mode. The dominant contribution then comes from the other two modes being sub-Hubble. Its scaling is $k_3^2/\mathcal{H}^2 \times k_1 k_2/k_D^2$, which leads to the above suppression when the short modes are of order k_D .

4 Evolution of μ -type spectral distortion

We are now ready to discuss the evolution of the chemical potential after the end of the μ -era, and how it contributes to the μT correlator. As we have seen in the previous section, μ is sourced by perturbations close to the damping scale, which is much shorter than the Hubble radius. We will denote these short scales with a subscript S . Consider then a long wavelength ζ_L mode, denoted by a subscript L , well outside the Hubble radius at the time η_f of the end of the μ -era, but inside the Hubble radius today. We know that its effect on short-scale perturbations sourcing μ , at zeroth and linear order in the gradients of this long mode, will be equivalent to that of a coordinate transformation (see, *e.g.*, [7, 44]). More precisely, we start by focusing on the zeroth order in gradients. We will discuss the general case at the end of the section.

4.1 From CFC to global coordinates

As we discussed in Section 2.2, the calculation of short-long mode coupling during the μ -era is most easily performed in local (CFC) coordinates. On the other hand, eventually the long mode re-enters the Hubble radius and induces the modulation in T and μ which we aim to measure. Therefore, at some point before observation, we have to change from CFC to global coordinates to account for how the long mode affect the propagation of the photons we eventually observe. We choose to do so at the end of the μ -era, corresponding to conformal time $\eta = \eta_f$. Using the fact that we are deeply into radiation dominance, the coordinate change from CFC to global coordinates reads as [22, 23, 28, 32]

$$\tilde{\eta} = \left(1 - \frac{\zeta_L}{3}\right)\eta, \quad (4.1a)$$

$$\tilde{\mathbf{x}} = (1 + \zeta_L)\mathbf{x}, \quad (4.1b)$$

where the long mode ζ_L is absent in the $\tilde{\mathbf{x}}$ coordinates.¹⁰ After this transformation, the metric takes the form

$$ds^2 = a^2(\eta) [-e^{2\Phi} d\eta^2 + e^{-2\Psi} d\mathbf{x}^2], \quad (4.2)$$

with

$$\Phi = \Phi_S - \frac{2\zeta_L}{3} - \frac{\eta\zeta_L}{3} \frac{\partial\Phi_S}{\partial\eta} + \zeta_L x^i \frac{\partial\Phi_S}{\partial x^i}, \quad (4.3a)$$

$$\Psi = \Psi_S - \frac{2\zeta_L}{3} - \frac{\eta\zeta_L}{3} \frac{\partial\Psi_S}{\partial\eta} + \zeta_L x^i \frac{\partial\Psi_S}{\partial x^i}. \quad (4.3b)$$

i.e. we recognize the Poisson gauge with no vector or tensor modes. Under the change of coordinates of Eqs. (4.1), μ_S transforms as a scalar. More precisely, we have

$$\mu = \mu_S - \frac{\eta\zeta_L}{3} \frac{\partial\mu_S}{\partial\eta} + \zeta_L x^i \frac{\partial\mu_S}{\partial x^i}. \quad (4.4)$$

¹⁰We note that these formulas for the so-called adiabatic mode have been derived considering the universe as composed of a single perfect fluid, *i.e.* neglecting viscosity, which is indeed negligible on very large scales.

Given that the conservation of μ_S after η_f implies $\frac{\partial \mu_S}{\partial \eta} = 0$, we will drop the time derivative in Eq. (4.4). The fluid velocity U^μ , instead, takes the form [23]

$$v^i = v_S^i - \frac{\eta \zeta_L}{3} \frac{\partial v_S^i}{\partial \eta} + \zeta_L x^j \frac{\partial v_S^i}{\partial x^j} , \quad (4.5)$$

where $U^i = e^\Psi v^i/a$. We see that, since we stop at zeroth order in the gradients of ζ_L , no large-scale velocity is generated.

Eqs. (4.3), (4.4), (4.5) give us the initial condition for the evolution of $\mu(\eta_f, \mathbf{x}_f)$ on the hypersurface $\eta = \eta_f$, when μ stops being created, up to the observer at (η_0, \mathbf{x}_0) .

4.2 Non-linear evolution

Let us now assume that the evolution from the end of the μ -era up to the last-scattering surface is dictated by the conservation of μ along the fluid lines (we generalize this in Appendix B). That is, until recombination the chemical potential satisfies the equation

$$U^\rho \nabla_\rho \mu = 0 . \quad (4.6)$$

After decoupling, the evolution is dictated only by the conservation of μ along the photon geodesics. Indeed, while the CMB temperature at recombination experiences an additional redshift E_0/E_{rec} as the photons travel from the last scattering surface to us (which is the source of the Sachs-Wolfe, integrated Sachs-Wolfe and Doppler effects), μ is immune to this effect. In fact, the solution to the collisionless Boltzmann equation $\frac{Df}{d\lambda} = 0$ (where λ is an affine parameter along the photon geodesics) is given by

$$\frac{2}{e^{\frac{E_{\text{rec}}}{T_{\text{rec}}} + \mu_{\text{rec}}} - 1} = \frac{2}{e^{\frac{E_0}{T_0} + \mu_0} - 1} , \quad (4.7)$$

where we used the Bose-Einstein expression for the photon distribution function, with E being the photon energy for an observer at rest with respect to the CMB frame (who coincides with the an observer comoving with the fluid during the tight-coupling regime). Since the equality must hold for all values of the photon energy, we obtain (for the temperature-only case, see also Appendix A of both [23] and [28])

$$T_0 = \frac{E_0}{E_{\text{rec}}} T_{\text{rec}} , \quad \mu_0 = \mu_{\text{rec}} . \quad (4.8)$$

We stress that this relation holds to all orders in cosmological perturbations, since it is just a consequence of Liouville's theorem.

The presence of the long mode will perturb the fluid lines and the photon trajectories, and with them the expression of the spatial coordinates on the η_f hypersurface in terms of the coordinates at the observation point:

- At linear order in the long mode, the solution for the fluid lines would take the form $x^i(t) = x^i + \int_{t_f}^t ds v_L^i(s, \mathbf{x})$. However, as we see in Eq. (4.5), v_L^i vanishes at zeroth order in gradients, so that $\mathbf{x}_f = \mathbf{x}_{\text{rec}}$.
- After decoupling, the solution of the geodesic equation at linear order in the long mode gives [23]

$$\mathbf{x}_{\text{rec}}(\hat{\mathbf{n}}) = \mathbf{x}_0 + \hat{\mathbf{n}}(\eta_0 - \eta_{\text{rec}}) + 2\hat{\mathbf{n}} \int_{\eta_{\text{rec}}}^{\eta_0} d\eta \Phi_L(\eta, \mathbf{x}_\eta) - 2 \int_{\eta_{\text{rec}}}^{\eta_0} d\eta (\eta - \eta_{\text{rec}}) \nabla_\perp \Phi(\eta, \mathbf{x}_\eta) , \quad (4.9)$$

where $\hat{\mathbf{n}}$ is the direction of observation, the time integrals are along the unperturbed photon trajectory $\mathbf{x}_\eta = \hat{\mathbf{n}}(\eta_0 - \eta)$, and ∇_\perp denotes a derivative perpendicular to the line of sight, $\nabla_i^\perp = (\delta_{ij} - \hat{n}_i \hat{n}_j) \partial_j$. Since $\mathbf{x}_f = \mathbf{x}_{\text{rec}}$, Eq. (4.9) provides the relation between \mathbf{x}_0 and \mathbf{x}_f and, with it, the relation between the inhomogeneities in μ at the end of the μ -era to the anisotropies in μ seen in the sky today.

To summarize, combining Eq. (4.9) with Eq. (4.4) we obtain the full solution for $\mu(t_0, x_0)$ at the observer's point, *i.e.*

$$\mu(\eta_0, x_0) = \mu_S(\eta_f, \mathbf{x}_{\text{rec}}) - \frac{3}{2} \Phi_L(\eta_f, \mathbf{x}_{\text{rec}}) \hat{\mathbf{n}} \cdot \nabla_{\hat{\mathbf{n}}} \mu_S(\eta_f, \mathbf{x}_{\text{rec}}) , \quad (4.10)$$

where we used the zeroth-order geodesic equation, $\mathbf{x}_{\text{rec}} = \hat{\mathbf{n}}(\eta_0 - \eta_{\text{rec}})$, to rewrite $\mathbf{x}_f \cdot \nabla_{\mathbf{x}_f}$ in Eq. (4.4), and we used the fact that in radiation dominance on super-Hubble scales $\zeta_L = -3\Phi_L/2$. Moreover, if we focus on large angular scales $\ell \lesssim 100$, we can rewrite the long-wavelength Newtonian potential as $-9\Theta_L(\hat{\mathbf{n}})/2$, using the Sachs-Wolfe approximation.

The above solution for the observed μ anisotropies straightforwardly shows that the angular correlator $C_\ell^{\mu T}$ vanishes. Indeed, we have seen that the only effects of the long mode on the evolution after η_f is the modification of the relation between \mathbf{x}_0 and \mathbf{x}_f and the spatial derivative term coming from the effect of the long mode on the short modes at η_f , *i.e.* the second term on the right-hand side of Eq. (4.10). Consider then the ensemble average of $\langle \mu_S \rangle$ at η_f : since it does not depend on spatial coordinates, it is unaffected by Eqs. (4.9), (4.10). The expression for $\langle \mu T \rangle$, then, schematically reads

$$\langle \mu T \rangle \sim \langle \Theta_L \rangle \langle \mu_S \rangle + \langle \Theta_L^2 \rangle \nabla_{\hat{\mathbf{n}}} \langle \mu_S \rangle = \langle \Theta_L \rangle \langle \mu_S \rangle = 0 , \quad (4.11)$$

since $\langle \mu_S \rangle$ does not contain any long mode for Θ_L to correlate with. A more detailed proof of Eq. (4.11) is given in Appendix D.

As in [23], the result of Eq. (4.10) is valid if the long mode is outside the sound horizon at the end of the μ -era (but inside the Hubble radius today), and holds at zeroth order in an expansion in k_L/k_S , where $k_L \sim \ell/\eta_0$ is the long-wavelength temperature mode and $k_S \sim k_D(z_f) \simeq 50 \text{ Mpc}^{-1}$ is the damping scale at the end of the μ -era. We can now see that there are two very important differences with respect to the computation of squeezed CMB bispectrum $B_{\ell_L \ell_S \ell_S}$ of [23]:

- While the expression for $B_{\ell_L \ell_S \ell_S}$ of [23] holds only in the squeezed limit, Eq. (4.10) (and consequently Eq. (4.11)) is an expression for the *full* μT angular correlator.
- In the $B_{\ell_L \ell_S \ell_S}$ case the long mode needed to be outside the Hubble radius at recombination, limiting the validity of the calculation to $\ell_L \lesssim 100$. Here ℓ can be pushed up to $\ell \sim \mathcal{H}_f \eta_0 = \mathcal{O}(1500)$, since it is enough to consider the long mode to be outside the Hubble radius at the end of the μ -era.

4.3 First order in the gradient of the long mode and beyond

In this section we show that our results can be directly extended to include gradients of the long mode. While to derive the explicit solution of Eq. (4.10) we stopped at zeroth order in k_L/k_S , the equations Eqs. (4.6), (4.8) are non-perturbative in such expansion. The solutions to these equations, *i.e.* conservation of μ along the fluid lines up to the last-scattering surface, and along the photon geodesics up to the observer's point, always involve spatial derivatives of μ : once projected on the sky, then, these spatial derivatives turn into derivatives along the

direction of observation $\hat{\mathbf{n}}$,¹¹ so that they will vanish once we average over the short modes. This can be seen as a generalization of the intuitive argument put forward in Section 1. Therefore, we are limited only by how accurately Weinberg’s theorem describes the evolution of the chemical potential up to the end of the μ -era. As shown in [45–47] (see also [28]), Weinberg’s theorem can be extended to gradient order: *i.e.* also at this order the effect of the long mode on the short modes is equivalent to a coordinate transformation and, similarly to the discussion below Eq. (4.4), ζ_L couples only to spatial derivatives of μ_S . At order k_L^2/\mathcal{H}_f^2 , however, we cannot anymore use this argument: indeed, at this order the long mode is contributing to the local curvature, and this effect cannot be mimicked by a coordinate transformation. This is precisely the CFC result of Section 3.3.

Throughout this section we have assumed that after the end of the μ -era the evolution of the chemical potential is simply dictated by Eq. (4.6). However, as shown in [9], during the tight-coupling evolution up to the last-scattering surface inhomogeneities of μ on small scales will be damped. In Appendix B, we show that these effects do not give additional correlations with the long mode.

5 Observed μT cross-correlation

We have argued that the observed μT correlator receives no “projection” contributions from modes outside the Hubble radius during the μ -era up to corrections of order $k_L^2/\mathcal{H}_f^2 \ll 1$. In particular, these non-primordial effects have a different k dependence (and therefore ℓ dependence in angular correlators) from local non-Gaussianity. The above results were derived assuming the only source of μ production is Silk damping. In this section, we estimate also the production due to heat conduction and compare all contributions (like, *e.g.*, those from temperature non-linearities). After providing formulae for the observed μT angular correlator we show, by mean of a Fisher forecast, that the non-primordial contributions do not need to be computed because marginalizing over them does not appreciably change the constraints of f_{NL} even for a very futuristic cosmic variance-limited experiment.

5.1 Contributions to the observed $\langle \mu T \rangle$

We consider three types of non-primordial corrections, namely $\langle \mu^{(3)} T^{(1)} \rangle$, $\langle \mu^{(2)} T^{(2)} \rangle$, and $\langle \mu^{(1)} T^{(1)} \rangle$. In the following, we discuss these remaining sources separately, estimating their size and finding which one gives the strongest contribution. All of these effects must then be compared to the signal we are interested in, *i.e.* local non-Gaussianity from multi-field inflation (or any model that violates the consistency relation). For simplicity, we estimate and compare all contributions to the $\langle \mu T \rangle$ correlator evaluated at the last-scattering surface, $\eta = \eta_{\text{rec}}$. We find that the largest non-primordial contribution to μT , *i.e.* the leading contribution in a single-field universe obeying the consistency relation, comes from μ production at third order, discussed in Section 3.3.

Local non-Gaussianity

We find it convenient to discuss the size of any non-primordial contribution to μT in terms of an *effective* f_{NL} . Therefore here we briefly review the contribution of (multi-field) local

¹¹We can see this by using the solution of Eq. (4.9), *i.e.* $\mathbf{x}_{\text{rec}}(\hat{\mathbf{n}}) = \mathbf{x}_0 + \hat{\mathbf{n}}(\eta_0 - \eta_{\text{rec}})$ on the background.

non-Gaussianity to μT , defined as¹²

$$\langle \zeta(\mathbf{k}_1)\zeta(\mathbf{k}_2)\zeta(\mathbf{k}_3)' \rangle = \frac{6f_{\text{NL}}}{5} [P_\zeta(k_1)P_\zeta(k_2) + 2 \text{ perms.}] , \quad (5.1)$$

where we use a prime to denote that we have factored out a delta function $(2\pi)^3\delta^{(3)}(\sum_i \mathbf{k}_i)$ of momentum conservation. Since μ_S starts quadratic in ζ , at first order in f_{NL} the bispectrum of Eq. (5.1) leads to a contribution to $\langle \mu T \rangle$ of the form (c.f. Eq. (16) in [3], and the computation in Appendix F)

$$\begin{aligned} \langle \mu(\mathbf{x})T(\mathbf{y}) \rangle &= \int_{\mathbf{q}_1, \mathbf{q}_2, \mathbf{k}} \langle \mu_S(\mathbf{q}_1 - \mathbf{k}, \mathbf{k})T(\mathbf{q}_2) \rangle e^{i(\mathbf{q}_1 \cdot \mathbf{x} + \mathbf{q}_2 \cdot \mathbf{y})} \\ &\sim f_{\text{NL}} \langle \mu_S \rangle \int_{\mathbf{q}} P_\zeta(q) \Delta^T(q) e^{i\mathbf{q} \cdot (\mathbf{x} - \mathbf{y})} , \end{aligned} \quad (5.2)$$

where $\Delta^T(q)$ is the transfer function that relates ζ to temperature fluctuations at the time of last-scattering (we neglect the equivalent for μ , responsible for the damping of μ fluctuations, since it does not affect our estimates). Its Fourier transform then reads

$$\langle \mu(\mathbf{q})T(-\mathbf{q}) \rangle'_{\text{NG}} \sim f_{\text{NL}} \langle \mu_S \rangle P_\zeta(q) \Delta^T(q) . \quad (5.3)$$

μ production at third order

As outlined in Section 4, any mode coupling that is induced between long modes and μ_S after the μ -era drops out of the μT correlator. The leading contribution therefore comes from the second derivative of the long mode during the μ -era, which is locally equivalent to a spatial curvature and modulates the amount of distortion that is produced. The relevant cubic term $\mu^{(3)}$ was estimated in Section 3.3 to be

$$\mu^{(3)}(\eta, \mathbf{x}) = -b_1 \frac{\partial^2 \zeta_L(\eta, \mathbf{x})}{\mathcal{H}_f^2} \langle \mu_S \rangle . \quad (5.4)$$

Its contribution to the correlator is then given by

$$\langle \mu^{(3)}(\mathbf{q})T^{(1)}(-\mathbf{q}) \rangle' = b_1 \left(\frac{q}{\mathcal{H}_f} \right)^2 P_\zeta(q) \Delta^T(q) \langle \mu_S \rangle + \mathcal{O}(q^3) . \quad (5.5)$$

Second-order temperature corrections

Here we provide a rough estimate of second order effects in temperature $T^{(2)}$. Given that these are found to be very small corrections, we are cavalier about the second-order transfer function and simply use the rough approximation $T = T^{(1)} + (T^{(1)})^2$. This contributes as

$$\begin{aligned} \langle \mu^{(2)}(\mathbf{x})T^{(2)}(\mathbf{y}) \rangle &= \int_{\mathbf{q}_1, \mathbf{q}_2, \mathbf{k}_1, \mathbf{k}_2} \langle W(\mathbf{q}_1 - \mathbf{k}_1, \mathbf{k}_1) \zeta(\mathbf{q}_1 - \mathbf{k}_1) \zeta(\mathbf{k}_1) T(\mathbf{q}_2 - \mathbf{k}_1) T(\mathbf{k}_2) \rangle \\ &\quad \times e^{i(\mathbf{q}_1 \cdot \mathbf{x} + \mathbf{q}_2 \cdot \mathbf{y})} \\ &= \int_{\mathbf{q}} \int_{\mathbf{k}} W(|\mathbf{q} - \mathbf{k}|, k) P_\zeta(|\mathbf{q} - \mathbf{k}|) \Delta^T(|\mathbf{q} - \mathbf{k}|) e^{i\mathbf{q} \cdot (\mathbf{x} - \mathbf{y})} P_\zeta(k) \Delta^T(k) , \end{aligned} \quad (5.6)$$

¹²Notice that, since we are working in CFC, f_{NL} equals zero in single-field cosmologies.

where W indicates the window function of Eq. (3.8), which contains a two derivative suppression factor when at least one of the arguments is small. Fourier transforming, we thus find

$$\langle \mu^{(2)}(\mathbf{q}) T^{(2)}(-\mathbf{q}) \rangle' = \int_{\mathbf{k}} W(|\mathbf{q} - \mathbf{k}|, k) P_{\zeta}(|\mathbf{q} - \mathbf{k}|) \Delta^T(|\mathbf{q} - \mathbf{k}|) P_{\zeta}(k) \Delta^T(k) . \quad (5.7)$$

We now show that this is subdominant with respect to $\langle \mu^{(3)} T^{(1)} \rangle$. Let us separate the integral into modes longer than the suppression scale during μ and those of order $q_{\text{eff}} \equiv \sqrt{\mathcal{H}_f k_D}$, which is roughly the scale at which the window function qualitatively changes behavior. Then, dropping some $\mathcal{O}(1)$ numbers in the window function, we find

$$\begin{aligned} \langle \mu^{(2)}(\mathbf{q}) T^{(2)}(-\mathbf{q}) \rangle'_{\text{long}} &\sim \int_{\mathbf{k}, k \ll q_{\text{eff}}} P_{\zeta}(|\mathbf{q} - \mathbf{k}|) \Delta^T(|\mathbf{q} - \mathbf{k}|) P_{\zeta}(k) \Delta^T(k) \left(\frac{|\mathbf{q} - \mathbf{k}|}{q_{\text{eff}}} \right)^2 \left(\frac{k}{q_{\text{eff}}} \right)^2 \\ &\sim \Delta_{\zeta}^2(q) P_{\zeta}(q) (\Delta^T(q))^2 \left(\frac{q}{q_{\text{eff}}} \right)^4 , \end{aligned} \quad (5.8)$$

where we used $k \sim q$. The remaining part takes the form

$$\begin{aligned} \langle \mu^{(2)}(\mathbf{q}) T^{(2)}(-\mathbf{q}) \rangle'_{\text{short}} &\sim \int_{\mathbf{k}, k \sim q_{\text{eff}}} \Delta^T(|\mathbf{q} - \mathbf{k}|) P_{\zeta}(|\mathbf{q} - \mathbf{k}|) \Delta^T(k) P_{\zeta}(k) \\ &\sim \Delta_{\zeta}^2(q_{\text{eff}}) P_{\zeta}(q_{\text{eff}}) (\Delta^T(q_{\text{eff}}))^2 . \end{aligned} \quad (5.9)$$

From this we can easily see that the long contribution of Eq. (5.8) is subdominant to the above contribution. Comparing the short contribution to μ production at third order we find

$$\frac{\langle \mu^{(2)}(\mathbf{q}) T^{(2)}(-\mathbf{q}) \rangle'}{\langle \mu^{(3)}(\mathbf{q}) T^{(1)}(-\mathbf{q}) \rangle'} \sim \left(\frac{q}{q_{\text{eff}}} \right)^{-2} \left(\frac{\mathcal{H}_f}{q_{\text{eff}}} \right)^2 \frac{P_{\zeta}(q_{\text{eff}})}{P_{\zeta}(q)} \frac{\Delta^T(q_{\text{eff}})}{\Delta^T(q)} \lesssim \left(\frac{q}{q_{\text{eff}}} \right) \left(\frac{\mathcal{H}_f}{q_{\text{eff}}} \right)^2 \ll 1 , \quad (5.10)$$

where we use that $\langle \mu_S \rangle \sim \Delta_{\zeta}^2(q_D)$.

μ production at first order due to heat conduction

If we look at Eqs. (3.3), (3.4a), we can see that the creation of μ at linear order due to heat conduction is suppressed by two spatial derivatives. Indeed, we see that the contribution to the evolution of μ from heat conduction is a divergence of a vector orthogonal to the fluid lines, so that up to first order in perturbations it will be $\sim \partial^2 \zeta$ (see also Eq. (3.18) and Eq. (3.19) of [9]). The suppression scale for this effect is k_D^{-2} : the heat conduction coefficient is also proportional to the photon mean free path t_{γ} [9]. We therefore estimate its contribution from super-Hubble modes to be at most

$$\mu^{(1)}(\mathbf{q}) \sim \left(\frac{q}{k_D} \right)^2 R^2 \zeta(\mathbf{q}) , \quad (5.11)$$

where the baryon loading is $R = 3\bar{\rho}_b/(4\bar{\rho}_{\gamma})$. Inside the correlator this yields

$$\langle \mu^{(1)}(\mathbf{q}) T^{(1)}(-\mathbf{q}) \rangle' \sim \left(\frac{q}{k_D} \right)^2 R^2 P_{\zeta}(q) \Delta^T(q) . \quad (5.12)$$

Comparing this to the first contribution, we find

$$\frac{\langle \mu^{(1)}(\mathbf{q}) T^{(1)}(-\mathbf{q}) \rangle'}{\langle \mu^{(3)}(\mathbf{q}) T^{(1)}(-\mathbf{q}) \rangle'} \sim \frac{R^2}{\Delta_\zeta^2(k_D)} \left(\frac{\mathcal{H}_f}{k_D} \right)^2. \quad (5.13)$$

Now note that R at the end of the μ -era is approximately given by¹³

$$R = R_{\text{eq}} \frac{(1 + z_{\text{eq}})}{(1 + z_f)} \simeq \frac{1}{6} \frac{3 \times 10^3}{5 \times 10^4} \simeq 10^{-2}, \quad (5.14)$$

where again we have used that $\langle \mu_S \rangle \sim \Delta_\zeta^2(q_D)$. Since $\Delta_\zeta^2 \sim 10^{-9}$, the baryon suppression is clearly less than the additional perturbations, which forces us to compare the Hubble radius during the μ -era and the damping scale as well. At the end of the μ -era, $k_D \simeq 50 \text{ Mpc}^{-1}$ and Hubble rate is approximately 10^{-1} Mpc^{-1} . Hence the ratio is of order

$$\left(\frac{\mathcal{H}_f}{k_D} \right) \simeq 10^{-3}, \quad (5.15)$$

which means that the first order production is estimated to be 10 % of the cubic production. Notice that this number is not very small and quite a few assumptions went into this estimate, such as $b_1 = \mathcal{O}(1)$ and Eq. (5.11).

5.2 μT angular correlation and Fisher forecast

We have concluded that the largest contribution from non-linear evolution is the bias effect of Eqs. (3.9), (3.10). Let us now first translate our result into angular correlations and then compare it with the contribution coming from local non-Gaussianity. More precisely, we carry out a Fisher forecast on the detectability of f_{NL} by a full-sky cosmic variance-limited experiment that can measure μ anisotropies up to $\ell_{\text{max}} = 1000$ (a similar forecast for a noise-dominated PIXIE-like experiment is carried out in Appendix G).

In order to write down the likelihood, we need the expression for the decomposition of μ on the sky in spherical harmonics, *i.e.*

$$a_{\ell m}^\mu(\eta_0, \mathbf{x}) = 4\pi i^{-\ell} \int_{\mathbf{k}} e^{i\mathbf{k} \cdot \mathbf{x}} \mu(\eta_f, \mathbf{k}) \underbrace{e^{-k^2 \Delta q_{\mu,D}^{-2}} j_\ell(k \Delta \eta)}_{\equiv \Delta_\ell^\mu(k)} Y_{\ell m}^*(\hat{\mathbf{k}}), \quad (5.16)$$

where $\Delta \eta \equiv \eta_0 - \eta_{\text{rec}}$. We see that the expression for the μ transfer function $\Delta_\ell^\mu(k)$ contains two terms:

- First, we have the damping of μ inhomogeneities from the end of the μ -era to the last-scattering surface, *i.e.*

$$\mu(\eta_{\text{rec}}, \mathbf{k}) = \mu(\eta_f, \mathbf{k}) e^{-k^2 \Delta q_{\mu,D}^{-2}}, \quad (5.17)$$

where $\Delta q_{\mu,D}^{-2}$ is defined in terms of the dissipation scale $q_{\mu,D}$ of μ inhomogeneities as

$$\Delta q_{\mu,D}^{-2} \equiv [q_{\mu,D}^{-2}(z_{\text{rec}}) - q_{\mu,D}^{-2}(z_f)] \simeq q_{\mu,D}^{-2}(z_{\text{rec}}). \quad (5.18)$$

The expression for $q_{\mu,D}$ as a function of redshift has been derived in Eq. (4.8) of [9]: at recombination one has that $q_{\mu,D}^{-2}(z_{\text{rec}}) \simeq 0.084 \text{ Mpc}^{-1}$.

¹³Note that at earlier times, the comoving damping scale k_D increases faster than the conformal Hubble rate, which means that the baryon term is smaller at earlier times during the μ -era.

- Then, there is a spherical Bessel function of projection from the last-scattering surface to the observer at (η_0, \mathbf{x}) .

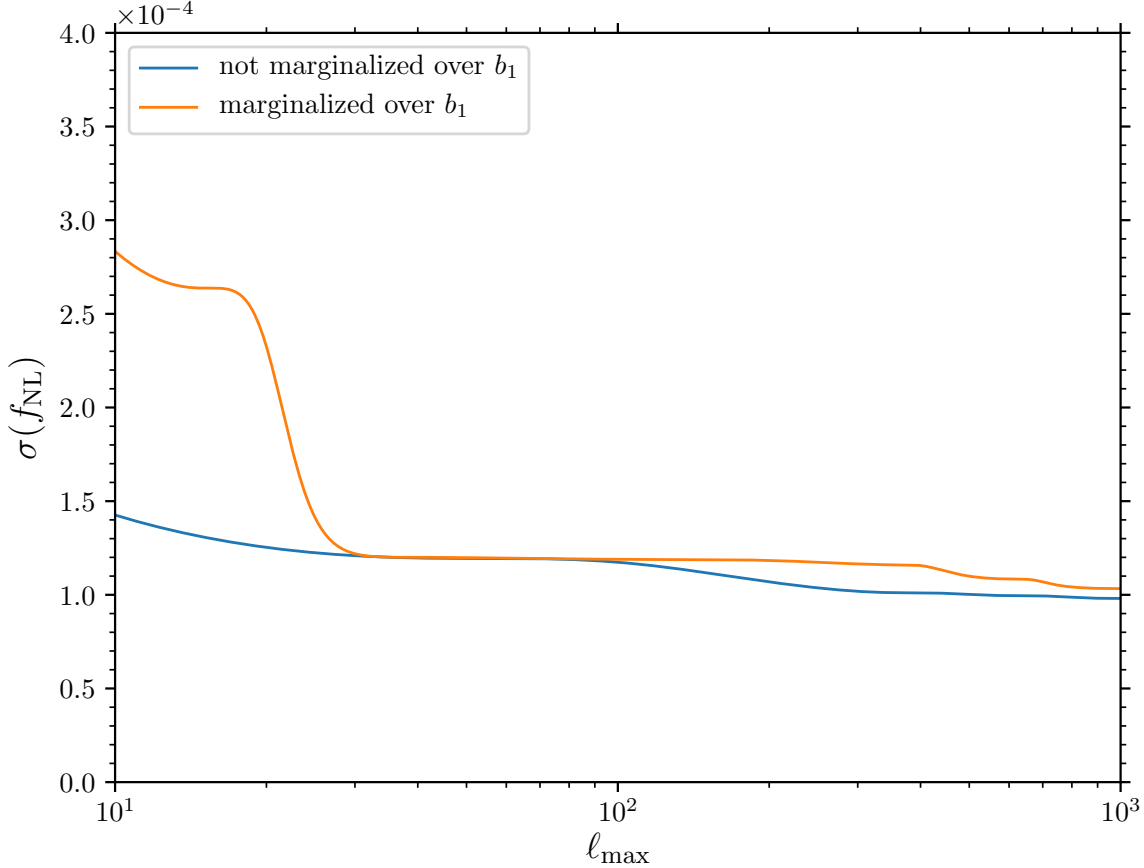


Figure 1: 1σ detection limits on f_{NL} for a full-sky cosmic variance-limited experiment as a function of ℓ_{max} . We see that marginalizing over the bias parameter b_1 does not significantly affect $\sigma(f_{\text{NL}})$, especially if modes $\ell \gtrsim 20$ are accessible.

With the expression for the harmonic coefficients of Eq. (5.16) at hand, we can compute the likelihood in terms of the angular correlators $C_\ell^{\mu T}$, $C_\ell^{\mu\mu}$ and C_ℓ^{TT} . The first two are computed in Appendix F, while we use CAMB [48] to obtain the latter. We start by defining

$$C_\ell^{\mu T}|_{f_{\text{NL}}} \equiv C_\ell^{\mu T}(f_{\text{NL}} = 1, b_1 = 0) , \quad (5.19a)$$

$$C_\ell^{\mu T}|_{b_1} \equiv C_\ell^{\mu T}(f_{\text{NL}} = 0, b_1 = 1) . \quad (5.19b)$$

Then, if we consider a full-sky cosmic variance-limited experiment, the logarithm of the likelihood reads

$$-2 \log \mathcal{L} = \sum_{\ell=2}^{\ell_{\text{max}}} \frac{(C_\ell^{\mu T})^2}{\sigma_\ell^2} = \sum_{\ell=2}^{\ell_{\text{max}}} (2\ell + 1) \frac{(f_{\text{NL}} C_\ell^{\mu T}|_{f_{\text{NL}}} + b_1 C_\ell^{\mu T}|_{b_1})^2}{C_\ell^{\mu\mu} C_\ell^{TT}} , \quad (5.20)$$

where we have chosen a zero fiducial value for f_{NL} and b_1 (indeed, we are interested in upper limits: moreover $C_{\ell}^{\mu T}$ is linear in f_{NL} and b_1 , so taking a non-zero fiducial would not affect the Fisher matrix), and we used the fact that, if experimental noise is negligible, the variance of $C_{\ell}^{\mu T}$ is given by

$$\sigma_{\ell}^2 = \langle (C_{\ell}^{\mu T})^2 \rangle - \langle C_{\ell}^{\mu T} \rangle^2 = \frac{C_{\ell}^{\mu\mu} C_{\ell}^{TT}}{2\ell + 1}. \quad (5.21)$$

It is now straightforward to derive the 1σ errors on f_{NL} from Eq. (5.20): the Fisher matrix is defined by

$$F_{ij} = -\frac{\partial^2 \log \mathcal{L}}{\partial p_i \partial p_j} \quad (p_1 = f_{\text{NL}}, p_2 = b_1), \quad (5.22)$$

and the unmarginalized and marginalized 1σ errors are, respectively, given by

$$\sigma(f_{\text{NL}})|_{\text{unmarg.}} = \frac{1}{\sqrt{F_{11}}}, \quad (5.23a)$$

$$\sigma(f_{\text{NL}})|_{\text{marg.}} = \sqrt{(F^{-1})_{11}}. \quad (5.23b)$$

These are shown in Fig. 1: we see that marginalizing over the bias parameter does not degrade the detection limit for f_{NL} , which is of the order of 10^{-4} for $\ell_{\text{max}} > 20$.¹⁴ This had to be expected, since the effect of spatial curvature on μ production scales very differently in the squeezed limit with respect to local non-Gaussianity. Also, we notice that the unmarginalized 1σ detection limit on f_{NL} is 1.2×10^{-4} , which is smaller than the one originally quoted in [3]: the reason is that there the smearing scale was conservatively taken to be $k_{\text{D}}(z_f)$. Here, following [9], we instead take it to be $k_{\text{D}}(z_{\text{rec}})$.

6 Discussion and conclusions

In this work, we studied the prediction for the angular correlator $C_{\ell}^{\mu T}$ between CMB μ -type spectral distortions and temperature anisotropies in single-field, attractor inflation. We found that the leading term comes from the non-linear effect of a long curvature mode on the *production* of μ distortions. We estimate this effect to be of order $b_1 k^2 / \mathcal{H}_f^2$, where $\mathcal{H}_f \simeq 10^{-1} \text{ Mpc}^{-1}$ is the Hubble radius at the end of the μ -era and $b_1 = \mathcal{O}(1)$ is a bias parameter. Since this contribution shows the scaling with k_L typical of the equilateral shape in the squeezed limit, it does not significantly affect searches for local non-Gaussianity as long as observations cover a few tens of ℓ . To make this more precise, we carry out a forecast for a full-sky cosmic variance-limited experiment. We assume that b_1 is an unknown parameter which we marginalize over. If the experiment has access to modes $\ell \gtrsim 20$, the 1σ detection limit on f_{NL} remains equal to its unmarginalized value of 1.2×10^{-4} .

We conclude that any constraints on $C_{\ell}^{\mu T}$ in any foreseeable future are indeed direct constraints on the primordial local f_{NL} : any effect coming from late-time evolution has a different ℓ dependence and a negligible amplitude. This is in stark contrast with, for example, the CMB squeezed bispectrum, where non-primordial effects do lead to an observed local shape even in single-field attractor inflation.

Note that we have been able to extend our result for the μT cross-correlator up to very short scales ($\ell \sim 1500$), because our derivation relies only on the temperature mode being

¹⁴Note that this forecast does not include any prior on b_1 and relies on the shapes only. For a realistic prior ($|b_1| \lesssim 10$) we expect the effect of marginalization to be negligible even at low ℓ . We confirm this in Appendix G.

outside the Hubble radius at the end of the μ -era, which is a order of magnitude shorter than the Hubble radius at recombination. Related to this point, we notice that our work assumed an instantaneous transition from the μ -era to the y -era: however, we can quickly realize that dropping this assumption would not affect the final results. Indeed, assume that μ production does not stop instantaneously at z_f , but becomes negligible after some redshift $\tilde{z}_f \lesssim z_f$: then, we can just use Weinberg's theorem starting from \tilde{z}_f and proceed in the same way as we discussed in the main text. Now the effect of the long mode on μ production would be of order $k^2/\mathcal{H}^2(\tilde{z}_f) \gtrsim k^2/\mathcal{H}^2(z_f)$.

We conclude by emphasizing that in this work we have considered only the μT angular correlator: recently, it has been pointed out that the primordial bispectrum can be constrained also by looking at μE correlations [17], and correlations of temperature and polarization with y -type spectral distortions [4, 18]. More precisely, combining y and μ distortions offers a powerful way to constrain the running of non-Gaussianity at small scales [4, 15, 18]. In addition to this, the possibility of using angular three-point functions like $B_{\ell_1 \ell_2 \ell_3}^{TT\mu}$ has been considered as a probe of the primordial trispectrum [3, 13, 14]. It would be interesting to extend our results to these observables.

Acknowledgements

It is a pleasure to thank Nicola Bartolo, Marco Celoria, Jens Chluba, Paolo Creminelli, Eiichiro Komatsu, Michele Liguori, Mehrdad Mirbabayi, Andrea Ravenni and Fabian Schmidt for useful discussions. G. C. acknowledges support from the Starting Grant (ERC-2015-STG 678652) “GrInflaGal” of the European Research Council. D. vd W. and E. P. are supported by the Delta-ITP consortium, a program of the Netherlands Organization for Scientific Research (NWO) that is funded by the Dutch Ministry of Education, Culture and Science (OCW). This work is part of the research programme VIDI with Project No. 680-47-535, which is (partly) financed by the Netherlands Organisation for Scientific Research (NWO).

A Window function for μ from super-Hubble scales

In this appendix, we compute the solution to Eq. (3.6) for the generation of μ distortions from damping of acoustic waves and discuss what is the leading suppression on large scales (*i.e.* we see how the correct general-relativistic calculation leads to the scaling of Eq. (3.8)).

In presence of viscous corrections, μ changes along the fluid lines as

$$U^\nu \nabla_\nu \mu = \frac{8t_\gamma}{15(A_n - A_s)} \left(P_{(\mu}^\rho \nabla_{|\rho|} U_{\nu)} \nabla^\nu U^\mu - \frac{(\nabla_\mu U^\mu)^2}{3} \right). \quad (\text{A.1})$$

As the right-hand side of the above equation starts at second order in perturbations, we assume that also μ starts at this order. This can be easily seen if we rewrite Eq. (A.1) as

$$U^\nu \nabla_\nu \mu = \frac{8t_\gamma}{15(A_n - A_s)} \sigma_{\mu\nu} \sigma^{\mu\nu}, \quad (\text{A.2})$$

where the anisotropic stress $\sigma_{\mu\nu} \equiv P_{(\mu}^\rho \nabla_{|\rho|} U_{\nu)} - \frac{\nabla_\mu U^\rho}{3} P_{\mu\nu}$ vanishes in a FLRW spacetime.

Given some foliation t of spacetime, with normal n^μ to the constant- t hypersurfaces, one can decompose the fluid velocity U^μ as (see also Eq. (B.9))

$$U^\mu = \gamma(n^\mu + v^\mu), \quad (\text{A.3})$$

where v^μ satisfies $h^\mu_{\nu}v^\nu = v^\mu$ ($h_{\mu\nu}$ being the projector on constant- t hypersurfaces), and the γ factor has its usual special relativistic definition. It is then straightforward to see that up to first order in perturbations the anisotropic stress takes the form

$$\sigma_{\mu\nu} = K_{\mu\nu} + {}^{(3)}\nabla_{(\mu}v_{\nu)} + 2n_{(\mu}K_{\nu)\rho}v^\rho - \frac{(K + {}^{(3)}\nabla_\rho v^\rho)h_{\mu\nu}}{3} - \frac{2Kn_{(\mu}v_{\nu)}}{3}, \quad (\text{A.4})$$

where $K_{\mu\nu} = Hh_{\mu\nu} + \delta K_{\mu\nu}$ and ${}^{(3)}\nabla_\mu$ are, respectively, the extrinsic curvature and the covariant derivative on constant- t hypersurfaces. Working in Newtonian gauge and dropping vector and tensor modes, *i.e.*

$$ds^2 = -(1 + 2\Phi)dt^2 + a^2(1 - 2\Psi)d\mathbf{x}^2, \quad (\text{A.5})$$

simplifies Eq. (A.4) further. Indeed, using that $\delta K_{\mu\nu} = -(\dot{\Psi} + H\Phi)h_{\mu\nu}$ at first order in perturbations, *i.e.* $K_{\mu\nu} = \frac{K}{3}h_{\mu\nu}$, all terms involving the extrinsic curvature cancel. Therefore, we remain with

$$\sigma_{\mu\nu} = {}^{(3)}\nabla_{(\mu}v_{\nu)} - \frac{{}^{(3)}\nabla_\rho v^\rho)h_{\mu\nu}}{3}, \quad (\text{A.6})$$

so that

$$U^\nu\nabla_\nu\mu = \frac{8t_\gamma}{15(A_n - A_s)} \left[{}^{(3)}\nabla_{(\mu}v_{\nu)} {}^{(3)}\nabla^{(\mu}v^{\nu)} - \frac{{}^{(3)}\nabla_\mu v^\mu)^2}{3} \right]. \quad (\text{A.7})$$

Integrating Eq. (A.7) in time from t_i to t_f gives the total amount of μ distortions produced by damping of acoustic waves. The whole procedure is illustrated in more detail in the Section 3.2: here we just want to show that the generation of μ distortions is suppressed (as one would expect) when the wavelength of any of the two modes on the right-hand side of Eq. (A.6) becomes large. For simplicity we consider only the term $({}^{(3)}\nabla_\mu v^\mu)^2$. We can rewrite it in terms of the Newtonian potentials using the shift constraint equation (working at linear order in $t_\gamma \times \partial_\mu$, we can use the perfect fluid equations). Up to second order in perturbations we obtain

$$({}^{(3)}\nabla_\mu v^\mu)^2 = \frac{4M_{\text{Pl}}^4 H^2}{a^4(\rho + p)^2} (\partial^2\Phi)^2, \quad (\text{A.8})$$

so that Eq. (A.7) becomes

$$\frac{\dot{\mu}}{H} \sim \frac{t_\gamma}{H} \frac{(\partial^2\Phi)^2}{a^2\mathcal{H}^2}. \quad (\text{A.9})$$

At zeroth order in t_γ , Φ evolves as $\Phi(\eta, k) = -2\zeta(k)j_1(x)/x$, with $x = k\eta/\sqrt{3}$ during radiation dominance. Using this solution in Eq. (A.9), we obtain

$$\frac{\dot{\mu}}{H} \sim \frac{1}{\sigma_T n_e a \mathcal{H}} \frac{k^2 q^2}{\mathcal{H}^2} \zeta(k) \zeta(q) \text{ for } k, q \rightarrow 0. \quad (\text{A.10})$$

We can further simplify this by using the approximate expression $k_D^{-1} \simeq \sqrt{\eta/\sigma_T n_e a} = \sqrt{1/\sigma_T n_e a \mathcal{H}}$ for the damping scale [41], *i.e.* $k_D^2 \simeq \sigma_T n_e a \mathcal{H}$. Then, we have

$$\frac{\dot{\mu}}{H} \sim \frac{k^2 q^2}{\mathcal{H}^2 k_D^2} \zeta(k) \zeta(q) \text{ for } k, q \rightarrow 0. \quad (\text{A.11})$$

This makes clear that very long-wavelength modes of ζ do not dissipate. More precisely, the leading contribution to $\dot{\mu}$ will be suppressed: taking the short modes to be inside the Hubble

radius, we see that the μ production is still suppressed by kq/k_D^2 , making the generation of μ distortions from viscosity a process active for $k \gtrsim k_D$ only. This result tells us that, since perturbations longer than the damping scale do not contribute to μ , it is possible to treat the effect on μ production of a long-wavelength (that re-enters the Hubble radius at the end of the μ -era) ζ mode as we did in Section 4, *i.e.* by an expansion in k_L/k_S , with $k_S \sim k_D(z_f) \simeq 50 \text{ Mpc}^{-1}$.

Writing v^μ in terms of the velocity potential v , *i.e.* $v^i = a^{-2} \partial_i v$ in Newtonian gauge [40], we can rewrite Eq. (A.7) as

$$\dot{\mu} = \frac{8t_\gamma a^{-4}}{15(A_n - A_s)} \left[(\partial_i \partial_j v)^2 - \frac{(\partial^2 v)^2}{3} \right]. \quad (\text{A.12})$$

We can then insert the linear transfer function for the velocity potential during radiation domination, *i.e.*

$$v(k) = \frac{T_v(\eta, k)\zeta(k)}{H}, \quad (\text{A.13})$$

where we added the Hubble for dimensional consistency. This is related to the standard transfer function for the Newtonian potential, which is given by

$$\Phi(\eta, k) = -2\zeta(k) \left(\frac{\sin x - x \cos x}{x^3} \right), \quad (\text{A.14})$$

where $x = k\eta/\sqrt{3}$. Using the $0i$ Einstein equation for scalar perturbations in Newtonian gauge, *i.e.*

$$\frac{(\rho + p)v}{2M_{\text{Pl}}^2} = -H\Phi - \dot{\Phi}, \quad (\text{A.15})$$

we find

$$T_v(\eta, k) = \left[\left(\frac{\sin x - x \cos x}{x^3} \right) + \mathcal{H}^{-1} \partial_\eta \left(\frac{\sin x - x \cos x}{x^3} \right) \right]. \quad (\text{A.16})$$

In momentum space we can write the formula for μ production as

$$\begin{aligned} \mu(\eta_f, \mathbf{x}) &= \frac{8}{15(A_s - A_n)} \int_{\mathbf{k}_1} \int_{\mathbf{k}_2} \zeta(\mathbf{k}_1) \zeta(\mathbf{k}_2) e^{i(\mathbf{k}_1 + \mathbf{k}_2) \cdot \mathbf{x}} \\ &\quad \times \underbrace{\int_0^\infty dz' \left(\frac{t_\gamma}{\mathcal{H}} \right) \left(\frac{(\mathbf{k}_1 \cdot \mathbf{k}_2)^2 - \frac{1}{3} k_1^2 k_2^2}{\mathcal{H}^2} \right) T_v(z', k_1) T_v(z', k_2) \mathcal{J}_\mu(z')}_{= W(\mathbf{k}_1, \mathbf{k}_2)} . \end{aligned} \quad (\text{A.17})$$

We recall that $\frac{t_\gamma}{\mathcal{H}} \sim \frac{\partial k_D^{-2}}{\partial z}$, c.f. Eq. (3) in [3]. Here we have in mind the exponential suppression of perturbations on scales smaller than the damping scale, which restricts the momentum integrals, as in [3].

B From the μ -era to recombination

In this appendix, we argue that the tight-coupling evolution between the end of the μ -era and recombination [9] does not lead to a correction to Eq. (4.11). Indeed, viscosity affects only the *inhomogeneities* in the chemical potential, *i.e.* it does not have an effect on a *uniform* μ .

The presence of a long mode modifies local physics (*e.g.* it changes the local electron density and with it the damping scale), but this only leads to couplings of the form $\sim \zeta_L \partial_i \mu_S$: we are then in the same situation as in Section 4.1, where we argued that such terms do not contribute to μT cross-correlation. In this appendix we put this argument on more formal grounds.

As long as Compton scattering is efficient, the Boltzmann equation drives the photon distribution towards the equilibrium form. That is, the evolution of the chemical potential along the photon geodesics is dictated by

$$\frac{1}{E} \frac{D\mu}{d\lambda} = \frac{\mu - \mu_0}{t_\gamma} , \quad (\text{B.1})$$

where $E = -P_\mu U^\mu$ is the photon energy measured by an observer comoving with the fluid, and we defined the monopole μ_0 as (we refer to Appendix E for a more detailed discussion of how integrations over the photon direction can be performed in a general-covariant way)

$$\mu_0(x) = \int \frac{d\hat{\mathbf{m}}}{4\pi} \mu(x, \hat{\mathbf{m}}) , \quad (\text{B.2})$$

with m^μ being the photon direction as measured by the observer moving along the fluid lines, *i.e.* $P^\mu = E(U^\mu + m^\mu)$. We have neglected the quadrupole μ_2 in the collision term: indeed, as discussed in [9, 49], it will be suppressed in the tight-coupling regime (together with higher multipoles).

We then proceed by decomposing μ as a monopole plus a dipole: working non-perturbatively in cosmological perturbations, we can write

$$\mu = \mu_0 - 3m^\nu P_\nu^\rho \nabla_\rho \mu_1 , \quad (\text{B.3})$$

where $P^\mu_\nu \equiv \delta^\mu_\nu + U^\mu U_\nu$ is the projector on the instantaneous rest frame of the fluid and μ_0 and μ_1 are two scalars that we assume to start at second order in the short modes.¹⁵

Since μ does not depend on energy, the left-hand side of Eq. (E.1) reads as

$$\frac{1}{E} \frac{D\mu}{d\lambda} = U^\nu \nabla_\nu \mu + m^\nu \nabla_\nu \mu + \frac{P^\rho \nabla_\rho m^\nu}{E} P_\nu^\lambda \frac{\partial \mu}{\partial m^\lambda} . \quad (\text{B.4})$$

Expanding then the photon geodesic equation, with straightforward manipulations we can see that

$$P_\nu^\lambda \frac{P^\rho \nabla_\rho m^\nu}{E} = (m^\mu \theta_\mu + m^\mu m^\nu \theta_{\mu\nu}) m^\lambda - U^\mu \nabla_\mu U^\lambda - m^\mu \theta_\mu^\lambda , \quad (\text{B.5})$$

where we defined $\theta^\mu \equiv U^\nu \nabla_\nu U^\mu$, $\theta^{\mu\nu} \equiv P^{\mu\rho} \nabla_\rho U^\nu$. After plugging Eq. (B.3) and Eq. (B.5) in Eq. (B.4), we can extract two equations for μ_0 and μ_1 by taking moments, *i.e.* by integrating the equation in $\int \frac{d\hat{\mathbf{m}}}{4\pi} (m^\mu m^\nu \dots)$. Since we have assumed that μ is composed by a monopole and a dipole, only the first two moments are needed. The final result is the system of coupled equations (see Appendix E)

$$U^\nu \nabla_\nu \mu_0 + 4\theta^\nu D_\nu \mu_1 - D_\nu D^\nu \mu_1 = 0 , \quad (\text{B.6a})$$

$$\frac{D^\nu \mu_0}{3} - \frac{4\theta^{(\nu\rho)} D_\rho \mu_1}{5} - \frac{2\theta D^\nu \mu_1}{5} + 3\theta^{\nu\rho} D_\rho \mu_1 - \theta^\nu U^\rho \nabla_\rho \mu_1 - D^\nu (U^\rho \nabla_\rho \mu_1) = \frac{D^\nu \mu_1}{t_\gamma} , \quad (\text{B.6b})$$

¹⁵Notice that μ_1 must have dimensions of an inverse energy, since μ is dimensionless: one could define $\mu = \mu_0 - 3t_\gamma m^\nu P_\nu^\rho \nabla_\rho \mu_1$ to make μ_1 dimensionless, but this is irrelevant for the discussion in this section since we integrate out μ_1 .

where have denoted the projection of the covariant derivative in the instantaneous rest frame of the fluid by D_μ (*i.e.* $D_\mu \sim P_\mu^\nu \nabla_\nu$). Notice that this is different from the covariant derivative on constant- η hypersurfaces, η being defined by Eqs. (4.1), (4.2).

B.1 Leading order

We start by approaching Eqs. (B.6) with the same method that we used to arrive at Eq. (4.10) (the general case will be discussed in Section B.2): since the two equations are linear in μ_0 and μ_1 , which we have assumed to start at second order in the short modes, we can consider the other tensors like U^μ , θ^μ , etc. to contain only the long mode ζ_L . If we drop all spatial derivatives of the long mode, θ^μ vanishes: indeed, as we discussed in Section 4, the large-scale spatial velocity v_L^i is zero at this order. Additionally, $\theta^{\mu\nu}$ is equal to $\theta P^{\mu\nu}/3$ at leading order in ζ_L . Then, if we take the three-divergence of Eq. (B.6b) (again neglecting spatial derivatives of ζ_L), we solve it for $U^\nu \nabla_\nu (D_\rho D^\rho \mu_1) = D_\rho D^\rho (U^\nu \nabla_\nu \mu_1) + \mathcal{O}(\partial_i \zeta_L)$, and plug the result back in the derivative of Eq. (B.6a) along U^μ , we arrive at

$$U^\nu \nabla_\nu (U^\rho \nabla_\rho \mu_0) - \frac{D_\nu D^\nu \mu_0}{3} - \left(\frac{\theta}{3} - \frac{1}{t_\gamma} \right) D_\nu D^\nu \mu_1 = 0. \quad (\text{B.7})$$

We can then solve algebraically for $D_\nu D^\nu \mu_1$ from Eq. (B.6a), plug the result in Eq. (B.7), and obtain an equation for the monopole μ_0 alone, *i.e.*

$$U^\nu \nabla_\nu (U^\rho \nabla_\rho \mu_0) - \frac{D_\nu D^\nu \mu_0}{3} - \left(\frac{\theta}{3} - \frac{1}{t_\gamma} \right) U^\nu \nabla_\nu \mu_0 = 0. \quad (\text{B.8})$$

Recalling that at the order we are working at there is no large scale velocity v_L^i , we can replace $D_\nu D^\nu \mu_0$ by ${}^{(3)}\nabla_\nu {}^{(3)}\nabla^\nu \mu_0$, *i.e.* with the covariant spatial derivative on the surfaces of constant time. Indeed, ${}^{(3)}\nabla_\mu \sim h_\mu^\nu \nabla_\nu$, where $h_{\mu\nu} = g_{\mu\nu} + n_\mu n_\nu$ is the projector on the constant- η surfaces. Since four-velocity of the fluid can be decomposed as

$$U^\mu = \gamma(n^\mu + v^\mu), \quad (\text{B.9})$$

where $\gamma^{-2} = 1 - h_{\mu\nu} v^\mu v^\nu$, we see that for vanishing v^μ the two projectors P_μ^ν and h_μ^ν coincide. Therefore, we can rewrite Eq. (B.8) as

$$U^\nu \nabla_\nu (U^\rho \nabla_\rho \mu_0) - \frac{{}^{(3)}\nabla_\nu {}^{(3)}\nabla^\nu \mu_0}{3} - \left(\frac{\nabla_\mu U^\mu}{3} - \frac{1}{t_\gamma} \right) U^\nu \nabla_\nu \mu_0 = 0. \quad (\text{B.10})$$

The relevant scales in Eq. (B.10) are H (from $\nabla_\mu U^\mu/3$), k^2 (from the three-dimensional Laplacian), and $t_\gamma^{-1} \sim k_D^2/(a\mathcal{H})$ (we use the approximate solution $k_D^2 \simeq a\mathcal{H}/t_\gamma$ for the damping scale [41]). Up to recombination the comoving damping scale k_D^{-1} is much shorter than \mathcal{H}^{-1} , therefore in the bracket multiplying $U^\nu \nabla_\nu \mu_0$ the second term dominates. Secondly, ${}^{(3)}\nabla_\nu {}^{(3)}\nabla^\nu \mu_0$ will be subleading with respect to this term if we look at correlations with temperature anisotropies that are longer than the damping scale at recombination. With these assumptions, we can effectively take the $t_\gamma \rightarrow 0$ limit of Eq. (B.10), finding

$$U^\nu \nabla_\nu \mu_0 = 0. \quad (\text{B.11})$$

The monopole created after the end of the μ -era is conserved along the fluid lines up to the last-scattering surface. This is nothing but Eq. (4.6), a key assumption in the analysis carried out in Section 4.

B.2 Subleading orders

As we are now going to discuss, however, it is also possible to use Eqs. (B.6) to make a statement more general than just a derivation of Eq. (4.6). Let us follow the results of Section 3 and assume that the initial dipole μ_1 vanishes, *i.e.* it is zero at the end of the μ -era.¹⁶ Therefore, we see that these *homogeneous* equations have a simple solution if the initial monopole is uniform. Indeed, for these initial conditions, the solution is

$$\mu_1 \equiv 0 \quad \text{and} \quad \mu_0 = \text{const.} \quad . \quad (\text{B.12})$$

In words, *only the inhomogeneities of the monopole evolve after the end of the μ -era*. We regard this as a generalization of the result of [9], that showed how the linear evolution up to recombination is a damping of the spatial fluctuations in the monopole.

One might wonder what happens if we relax the assumption of having the chemical potential *at recombination* consist of only a monopole. We can see that our conclusions will not be changed in the following way: the free-streaming solution will still be that of Eq. (4.8), since Eq. (4.7) must be satisfied for every value of the photon energy and both μ_0 and μ_1 in Eq. (B.3) do not depend on E . Then, let us consider the solution of Eq. (4.8) at zeroth order in the long modes (this is enough, since any “projection effect” interaction will be built from powers of ζ_L multiplying the zeroth-order solution, as we discussed in Section 4). We see that, using the fact that at this order m^μ is conserved along the photon geodesics (lensing begins at first order in perturbations), the contribution of the dipole to the full chemical potential at the observer’s point is of the form $\mu \sim \hat{\mathbf{n}} \cdot \nabla_{\hat{\mathbf{n}}} \mu_1$. This contribution vanishes once we average over the short modes, since $\langle \mu_1 \rangle$ does not depend on position (the proof is the same as the one in Appendix D).¹⁷

C Cancellation of $f_{\text{NL}} = 1 - n_s$ in global coordinates

In this appendix we comment on the relation of our result to Maldacena’s consistency condition for the squeezed bispectrum [7], which suggests a local f_{NL} of $1 - n_s$. In our result no such term appears. The reason is related to the discussion in the conclusions of [3]: Maldacena’s result is obtained in particular coordinates, which are not necessarily well-suited to compute observables. We stress that our derivation in the main text is more complete, coordinate-independent and exact up to the corrections discussed in Section 5.

$\langle \mu T \rangle$ in global coordinates

Using global coordinates in ζ gauge, the three-point function in single-field cosmology is given by [7]

$$\langle \zeta(\mathbf{q} \rightarrow 0) \zeta(\mathbf{k}) \zeta(-\mathbf{k}) \rangle' = -\frac{d \log k^3 P_\zeta(k)}{d \log k} P_\zeta(q) P_\zeta(k) \quad . \quad (\text{C.1})$$

¹⁶The μ -era happens deeply in the tight-coupling regime. The assumption of having multipoles beyond the monopole equal to zero during this epoch is just the assumption that μ production can be treated within the realm of fluid dynamics, *i.e.* by using Eq. (3.6).

¹⁷Equivalently, we cannot have a inhomogeneous average dipole $\langle \mu_1 \rangle$ if statistical isotropy is satisfied. This would amount to have a preferred vector $P_\nu^\rho \nabla_\rho \langle \mu_1 \rangle$ (see Eq. (B.3)).

If we combine this with the sub-Hubble expression for μ production, one naively concludes that there is a nonzero contribution to $\langle \mu T \rangle$ given by

$$\begin{aligned} \langle \mu(\mathbf{q}) T(-\mathbf{q}) \rangle' &\sim -(n_s - 1) \int_{k_D(z_f)}^{k_D(z_i)} d \log k \Delta_\zeta^2(k) P_\zeta(q) \\ &= \left\langle \int_{k_D(z_f)}^{k_D(z_i)} d \log k \Delta_{\zeta, G}^2(k(1 - \zeta_L)) \zeta(q) \right\rangle, \end{aligned} \quad (\text{C.2})$$

where the subscript “G” denotes the fact that this quantity is uncorrelated with the long mode. This last equality is the crucial observation in this context: Maldacena’s result can be interpreted as a local shift of coordinates in the presence of a long mode, see [28, 40]. Since μ is being created during this era, it is sensitive to a change of coordinates $\mu(t, \mathbf{x})$. This naive calculation is wrong, because it does not consistently use the same coordinates to describe every scale present in the computation. Namely, a local change of coordinates (simply a spatial dilation in ζ gauge [7, 44]) affects all local physics in the same way. In particular, the damping scale at the beginning and end of the μ -era is also slightly modified. Thus, the proper expression for the creation of μ in global coordinates is

$$\langle \langle \mu \rangle_{\zeta_L}(\mathbf{q}) T(-\mathbf{q}) \rangle' \propto \left\langle \int_{k_D(z_f) \times (1 - \zeta_L)}^{k_D(z_i) \times (1 - \zeta_L)} d \log (k(1 - \zeta_L)) \Delta_{\zeta, G}^2(k(1 - \zeta_L)) \zeta(q) \right\rangle = 0, \quad (\text{C.3})$$

where $\langle \mu \rangle_{\zeta_L}(\mathbf{q})$ denotes the expectation value of μ in the presence of a constant long mode. Substituting variables, we can simply remove any dependence of the short modes on the long modes, such that, after the μ -era, the correlation is zero indeed. The intuition is that regardless of which coordinates one uses, the total physical duration of the μ -era is always the same.

D Average μ distortions in the sky

In this appendix, we provide a more detailed proof of Eq. (4.11). As we have seen in Section 4, we can have two effects that involve the long-wavelength mode. First of all, its presence affects the relation between the direction of observation and the physical position at recombination. Then, it affects the observed μ anisotropies through the second term of Eq. (4.10), *i.e.* the effect of the long mode on the short modes at the end of the μ -era as obtained from Weinberg’s theorem, Eq. (4.4). Both effects involve derivatives of $\mu_S(\eta_f, \hat{\mathbf{n}}(\eta_0 - \eta_{\text{rec}}))$ with respect to $\hat{\mathbf{n}}$ (as can be checked by expanding $\mu_S(\eta_f, \mathbf{x}_{\text{rec}})$ at leading order in ζ_L): therefore, if the ensemble average of $\mu_S(\eta_f, \hat{\mathbf{n}}(\eta_0 - \eta_{\text{rec}}))$ is independent on the direction of observation, the final $C_\ell^{\mu T}$ will vanish. This is straightforward to see: indeed, from Section 3 we know that $\mu(\eta_f, \mathbf{x})$ can be written as (we will drop the subscript S for simplicity)

$$\mu(\eta_f, \mathbf{x}) = \int_{\mathbf{k}_1} \int_{\mathbf{k}_2} \zeta(\mathbf{k}_1) \zeta(\mathbf{k}_2) W(\mathbf{k}_1, \mathbf{k}_2) e^{i(\mathbf{k}_1 + \mathbf{k}_2) \cdot \mathbf{x}}. \quad (\text{D.1})$$

The free-streaming solution at zeroth order in ζ_L just corresponds to replacing \mathbf{x} with $\mathbf{x}_0 + \hat{\mathbf{n}}(\eta_0 - \eta_{\text{rec}})$, as seen in Eq. (4.9): therefore, when taking the ensemble average, the two momenta \mathbf{k}_1 and \mathbf{k}_2 are forced to be equal and opposite and any dependence on $\hat{\mathbf{n}}$ drops out.

E Moments of the Boltzmann equation

In this appendix, we collect some details of the calculations that lead to Eqs. (B.6). We recall that our starting equation for the evolution of the chemical potential is Eq. (B.1), *i.e.*

$$\frac{1}{E} \frac{D\mu}{d\lambda} = \frac{\mu - \mu_0}{t_\gamma} . \quad (\text{E.1})$$

In the above equation, E is the photon energy measured by the observer U^μ comoving with the fluid, and we assume that μ is only a function of the photon direction m^μ , defined by $P^\mu = E(U^\mu + m^\mu)$.

After expanding the derivative $\frac{D}{d\lambda}$ along the photon geodesics, as detailed in Section B, we can take moments of Eq. (E.1). As shown in [50] (see for example its Chapter 22) and Appendix A of [51], given a function $F = F(P^\mu, U^\nu, g_{\rho\sigma})$ we can integrate it over P^μ using the Lorentz-invariant measure $\frac{d^3P}{E(\mathbf{P})}$, where a local Lorentz frame in which $U^\mu = \delta_0^\mu$ is used to define the components of \mathbf{P} , and the positive-energy solution of $P_\mu P^\mu = -m^2$ is selected in the relation $E = E(\mathbf{P})$. For photons, this amounts to writing

$$m^\mu = (0, \sin \theta \cos \phi, \sin \theta \sin \phi, \cos \theta) , \quad (\text{E.2a})$$

$$E = |\mathbf{P}| \equiv P , \quad (\text{E.2b})$$

$$\frac{d^3P}{E(\mathbf{P})} = P dP \sin \theta d\theta d\phi . \quad (\text{E.2c})$$

In the case that the function F does not depend explicitly on E , as it is the case for both the left-hand and right-hand sides of Eq. (E.1), we can forget about the “radial” integration and write $\int d\phi d\theta \sin \theta \equiv \int d\hat{\mathbf{m}}$.¹⁸ With this result at hand, we also see that the definition of the monopole μ_0 as in Eq. (B.2) is now made rigorous.

On the left-hand side of Eq. (E.1), coming from the expansion of $\frac{D}{d\lambda}$, there will be many terms involving tensors orthogonal to the fluid velocity contracted with different powers of m^μ : here we collect some useful results that are needed to get the zeroth and first moments. Given a vector V^μ and a tensor $M^{\mu\nu}$, both orthogonal to U^μ (so that in the local Lorentz frame they will have only spatial components), we have that

$$\int \frac{d\hat{\mathbf{m}}}{4\pi} m^\mu V_\mu = 0 , \quad (\text{E.3a})$$

$$\int \frac{d\hat{\mathbf{m}}}{4\pi} m^\mu m^\nu M_{\mu\nu} = \frac{M_\mu^\mu}{3} , \quad (\text{E.3b})$$

$$\int \frac{d\hat{\mathbf{m}}}{4\pi} m^\mu m^\nu M_{\mu\nu} m^\rho V_\rho = 0 , \quad (\text{E.3c})$$

$$\int \frac{d\hat{\mathbf{m}}}{4\pi} m^\mu m^\nu V_\nu = \frac{V^\mu}{3} , \quad (\text{E.3d})$$

$$\int \frac{d\hat{\mathbf{m}}}{4\pi} m^\mu m^\nu m^\rho M_{\nu\rho} = 0 , \quad (\text{E.3e})$$

$$\int \frac{d\hat{\mathbf{m}}}{4\pi} m^\mu m^\nu m^\rho M_{\nu\rho} m^\lambda V_\lambda = \frac{2M^{(\mu\nu)}V_\nu + M_\nu^\nu V^\mu}{15} . \quad (\text{E.3f})$$

¹⁸Equivalently, integrating over P will give the same overall factor on both sides of Eq. (E.1).

F Details of the Fisher forecast

In this appendix, we collect some useful results that are needed to carry out the Fisher forecast of Section 5.2. As discussed in the main text, the expression for the decomposition of μ on the sky in spherical harmonics reads

$$a_{\ell m}^\mu(\eta_0, \mathbf{x}) = 4\pi i^{-\ell} \int_{\mathbf{k}} e^{i\mathbf{k}\cdot\mathbf{x}} \mu(\eta_f, \mathbf{k}) \Delta_\ell^\mu(k) Y_{\ell m}^*(\hat{\mathbf{k}}) , \quad (\text{F.1})$$

where

$$\Delta_\ell^\mu(k) = e^{-\frac{k^2}{q_{\mu, \text{D}}^2(z_{\text{rec}})}} j_\ell(k\Delta\eta) , \quad (\text{F.2})$$

with $\Delta\eta \equiv \eta_0 - \eta_{\text{rec}}$ and $q_{\mu, \text{D}}^2(z_{\text{rec}}) \simeq 0.084 \text{ Mpc}^{-1}$.

With this expression we can then readily compute the μT and the $\mu\mu$ angular correlators. We start by computing the two correlators $C_\ell^{\mu T}|_{f_{\text{NL}}}$ and $C_\ell^{\mu T}|_{b_1}$, which we have defined in Eq. (5.19). The general expression for the angular correlator is given by

$$\langle a_{\ell m}^\mu (a_{\ell' m'}^T)^* \rangle = (4\pi)^2 i^{-\ell+\ell'} \int_{\mathbf{a}} \int_{\mathbf{b}} e^{i(\mathbf{a}-\mathbf{b})\cdot\mathbf{x}} \langle \mu(\eta_f, \mathbf{a}) \zeta(-\mathbf{b}) \rangle \Delta_\ell^\mu(a) \Delta_{\ell'}^T(b) Y_{\ell m}^*(\hat{\mathbf{a}}) Y_{\ell' m'}(\hat{\mathbf{b}}) . \quad (\text{F.3})$$

In the squeezed limit we can write the ensemble average $\langle \mu(\eta_f, \mathbf{a}) \zeta(-\mathbf{b}) \rangle$ as

$$\langle \mu(\eta_f, \mathbf{a}) \zeta(-\mathbf{b}) \rangle' = \langle \mu(\eta_f, \mathbf{x}) \rangle P_\zeta(b) \left[\frac{12 f_{\text{NL}}}{5} + \frac{b_1 b^2}{\mathcal{H}_f^2} \right] , \quad (\text{F.4})$$

where $\langle \mu(\eta_f, \mathbf{x}) \rangle$ is obtained by taking the ensemble average of, *e.g.*, Eq. (3.7). Eq. (F.4), then, leads to

$$C_\ell^{\mu T}|_{f_{\text{NL}}} = \frac{24 \langle \mu \rangle}{5\pi} \int_0^{+\infty} db b^2 P_\zeta(b) \Delta_\ell^\mu(b) \Delta_\ell^T(b) , \quad (\text{F.5a})$$

$$C_\ell^{\mu T}|_{b_1} = \frac{2 \langle \mu \rangle}{\pi \mathcal{H}_f^2} \int_0^{+\infty} db b^4 P_\zeta(b) \Delta_\ell^\mu(b) \Delta_\ell^T(b) , \quad (\text{F.5b})$$

where we called $\langle \mu \rangle \equiv \langle \mu(\eta_f, \mathbf{x}) \rangle$ for simplicity of notation.

Then, we move to the computation of the $\mu\mu$ angular power spectrum. The steps of the calculation are similar to those above, *i.e.* we write

$$\langle a_{\ell m}^\mu (a_{\ell' m'}^{\mu'})^* \rangle = (4\pi)^2 i^{-\ell+\ell'} \int_{\mathbf{a}} \int_{\mathbf{b}} e^{i(\mathbf{a}-\mathbf{b})\cdot\mathbf{x}} \langle \mu(\eta_f, \mathbf{a}) \mu(\eta_f, -\mathbf{b}) \rangle \Delta_\ell^\mu(a) \Delta_{\ell'}^{\mu'}(b) Y_{\ell m}^*(\hat{\mathbf{a}}) Y_{\ell' m'}(\hat{\mathbf{b}}) . \quad (\text{F.6})$$

Now, however, we need to compute the Gaussian contribution to the ensemble average $\langle \mu(\eta_f, \mathbf{a}) \mu(\eta_f, -\mathbf{b}) \rangle$. Using Wick's theorem and working in the squeezed limit, it is straightforward to see that it is made up of a “connected” and a “disconnected” contribution:

$$\langle \mu(\eta_f, \mathbf{a}) \mu(\eta_f, -\mathbf{b}) \rangle = (2\pi)^6 \delta^{(3)}(\mathbf{a}) \delta^{(3)}(-\mathbf{b}) \langle \mu \rangle^2 + 2F(2\pi)^3 \delta^{(3)}(\mathbf{a} - \mathbf{b}) , \quad (\text{F.7})$$

where F is given by

$$F = \frac{1}{2\pi^2} \int_0^{+\infty} dk k^2 P_\zeta^2(k) W^2(k, k) . \quad (\text{F.8})$$

The disconnected one does not contribute to the angular correlator,¹⁹ while the connected one gives

$$C_\ell^{\mu\mu} = \frac{4F}{\pi} \int_0^{+\infty} db b^2 [\Delta_\ell^\mu(b)]^2. \quad (\text{F.9})$$

G Fisher forecast for a PIXIE-like experiment

In this appendix we carry out a forecast for a PIXIE-like experiment in a similar way to that of Section 5.2. We assume isotropic white noise, a 1σ uncertainty on the μ monopole of 10^{-8} and a Gaussian beam with a full-width-at-half-maximum $\theta_b = 1.6^\circ$ [3,8]. Correspondingly, we have that

$$C_\ell^{\mu\mu,\text{N}} = 4\pi \times 10^{-16} e^{\frac{\ell^2 \theta_b^2}{8\log 2}} = 4\pi \times 10^{-16} e^{\frac{\ell^2}{84^2}}, \quad (\text{G.1})$$

which is much larger than $C_\ell^{\mu\mu}$ [3]. Therefore, Eq. (5.20) becomes

$$-2 \log \mathcal{L} = \sum_{\ell=2}^{\ell_{\text{max}}} (2\ell + 1) \frac{(f_{\text{NL}} C_\ell^{\mu T} |_{f_{\text{NL}}} + b_1 C_\ell^{\mu T} |_{b_1})^2}{C_\ell^{\mu\mu,\text{N}} C_\ell^{TT}}. \quad (\text{G.2})$$

We can also study what happens if we add a physically-motivated prior on b_1 . We consider a (very conservative) Gaussian prior centered around $b_1 = 0$ and with $\sigma_{b_1} = 10$: the log-likelihood of Eq. (G.2), then, becomes

$$-2 \log \mathcal{L} = \sum_{\ell=2}^{\ell_{\text{max}}} (2\ell + 1) \frac{(f_{\text{NL}} C_\ell^{\mu T} |_{f_{\text{NL}}} + b_1 C_\ell^{\mu T} |_{b_1})^2}{C_\ell^{\mu\mu,\text{N}} C_\ell^{TT}} + \frac{b_1^2}{\sigma_{b_1}^2}. \quad (\text{G.3})$$

The results of the forecast are shown in Fig. 2. From the top panel we see that marginalizing over the bias parameter b_1 without any prior does not affect $\sigma(f_{\text{NL}})$ since PIXIE would be able to access modes with $\ell \gtrsim 20$. We also see that there is no improvement if we go to ℓ_{max} larger than $\mathcal{O}(100)$ since PIXIE does not have access to those scales, as shown in Eq. (G.1). In the bottom panel we show what happens if we include a prior on b_1 : we see that, in this case, even if we stop at scales $\ell_{\text{max}} \lesssim 20$ the different scale dependence of the two signals can be resolved. Consequently, marginalizing over b_1 does not affect $\sigma(f_{\text{NL}})$.

This confirms that the non-primordial effects are completely orthogonal to local non-Gaussianity and will not bias future constraints on f_{NL} in any way.

¹⁹Indeed, it forces both transfer functions in Eq. (F.6) to be evaluated at zero momentum, where they vanish for $\ell > 0$ (since $j_\ell(x) \sim x^\ell$ for $x \rightarrow 0$).

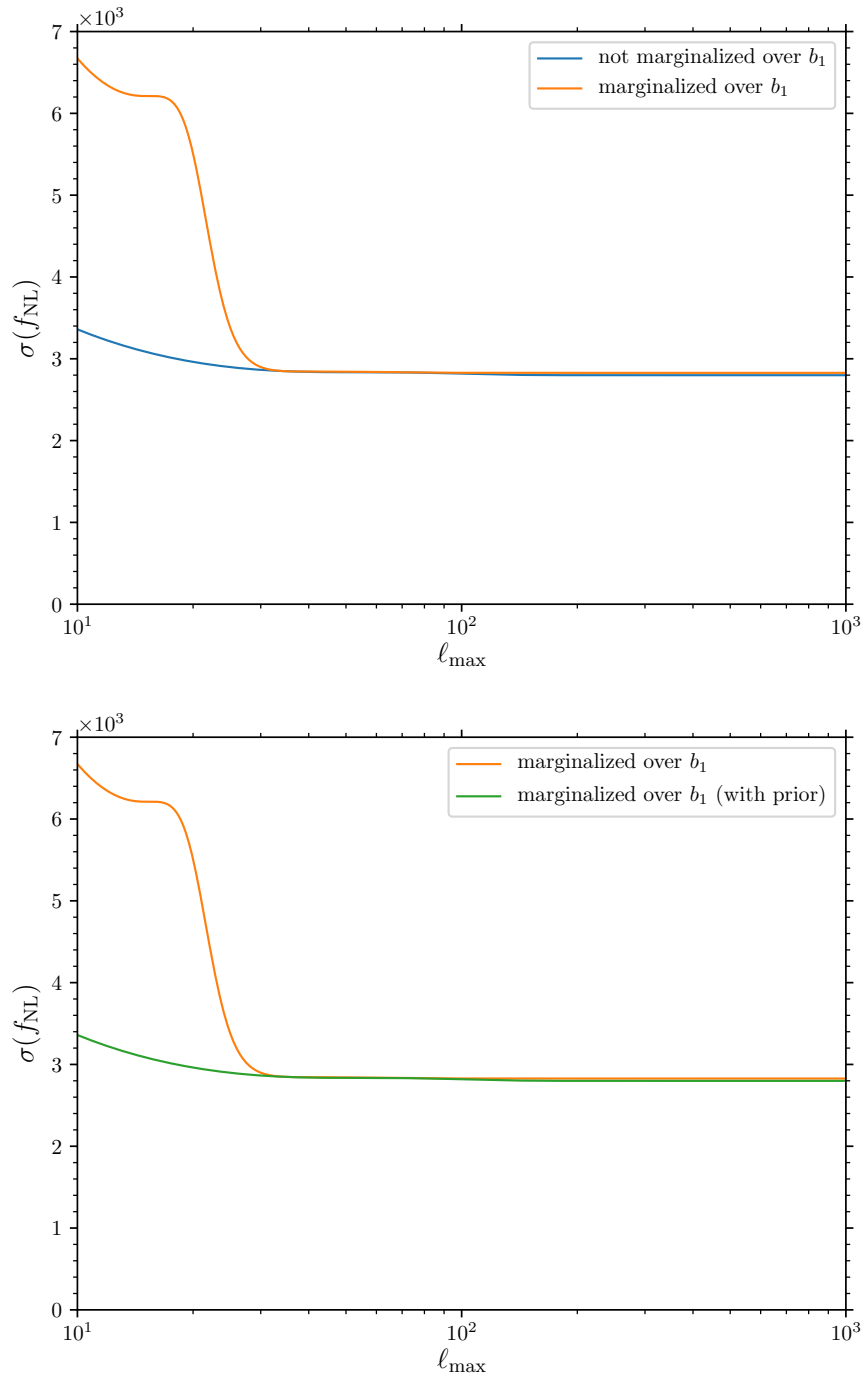


Figure 2: 1σ detection limits on f_{NL} for a PIXIE-like experiment as a function of ℓ_{max} . Top panel: same as Fig. 1. Bottom panel: added a Gaussian prior on b_1 .

References

- [1] W. Hu, D. Scott, and J. Silk, “Power spectrum constraints from spectral distortions in the cosmic microwave background,” *Astrophys. J.* **430** (1994) L5–L8, [arXiv:astro-ph/9402045 \[astro-ph\]](https://arxiv.org/abs/astro-ph/9402045).
- [2] J. Chluba, J. Hamann, and S. P. Patil, “Features and New Physical Scales in Primordial Observables: Theory and Observation,” *Int. J. Mod. Phys. D* **24** no. 10, (2015) 1530023, [arXiv:1505.01834 \[astro-ph.CO\]](https://arxiv.org/abs/1505.01834).
- [3] E. Pajer and M. Zaldarriaga, “A New Window on Primordial non-Gaussianity,” *Phys. Rev. Lett.* **109** (2012) 021302, [arXiv:1201.5375 \[astro-ph.CO\]](https://arxiv.org/abs/1201.5375).
- [4] R. Emami, E. Dimastrogiovanni, J. Chluba, and M. Kamionkowski, “Probing the scale dependence of non-Gaussianity with spectral distortions of the cosmic microwave background,” *Phys. Rev. D* **91** no. 12, (2015) 123531, [arXiv:1504.00675 \[astro-ph.CO\]](https://arxiv.org/abs/1504.00675).
- [5] E. Komatsu and D. N. Spergel, “Acoustic signatures in the primary microwave background bispectrum,” *Phys. Rev. D* **63** (2001) 063002, [arXiv:astro-ph/0005036 \[astro-ph\]](https://arxiv.org/abs/astro-ph/0005036).
- [6] N. Bartolo, E. Komatsu, S. Matarrese, and A. Riotto, “Non-Gaussianity from inflation: Theory and observations,” *Phys. Rept.* **402** (2004) 103–266, [arXiv:astro-ph/0406398 \[astro-ph\]](https://arxiv.org/abs/astro-ph/0406398).
- [7] J. M. Maldacena, “Non-Gaussian features of primordial fluctuations in single field inflationary models,” *JHEP* **05** (2003) 013, [arXiv:astro-ph/0210603 \[astro-ph\]](https://arxiv.org/abs/astro-ph/0210603).
- [8] J. Ganc and E. Komatsu, “Scale-dependent bias of galaxies and mu-type distortion of the cosmic microwave background spectrum from single-field inflation with a modified initial state,” *Phys. Rev. D* **86** (2012) 023518, [arXiv:1204.4241 \[astro-ph.CO\]](https://arxiv.org/abs/1204.4241).
- [9] E. Pajer and M. Zaldarriaga, “A hydrodynamical approach to CMB μ -distortion from primordial perturbations,” *JCAP* **1302** (2013) 036, [arXiv:1206.4479 \[astro-ph.CO\]](https://arxiv.org/abs/1206.4479).
- [10] A. Ota, T. Sekiguchi, Y. Tada, and S. Yokoyama, “Anisotropic CMB distortions from non-Gaussian isocurvature perturbations,” *JCAP* **1503** no. 03, (2015) 013, [arXiv:1412.4517 \[astro-ph.CO\]](https://arxiv.org/abs/1412.4517).
- [11] A. Naruko, A. Ota, and M. Yamaguchi, “Probing small-scale non-Gaussianity from anisotropies in acoustic reheating,” *JCAP* **1505** no. 05, (2015) 049, [arXiv:1503.03722 \[astro-ph.CO\]](https://arxiv.org/abs/1503.03722).
- [12] R. Khatri and R. Sunyaev, “Constraints on μ -distortion fluctuations and primordial non-Gaussianity from Planck data,” *JCAP* **1509** no. 09, (2015) 026, [arXiv:1507.05615 \[astro-ph.CO\]](https://arxiv.org/abs/1507.05615).
- [13] N. Bartolo, M. Liguori, and M. Shiraishi, “Primordial trispectra and CMB spectral distortions,” *JCAP* **1603** no. 03, (2016) 029, [arXiv:1511.01474 \[astro-ph.CO\]](https://arxiv.org/abs/1511.01474).
- [14] M. Shiraishi, N. Bartolo, and M. Liguori, “Angular dependence of primordial trispectra and CMB spectral distortions,” *JCAP* **1610** no. 10, (2016) 015, [arXiv:1607.01363 \[astro-ph.CO\]](https://arxiv.org/abs/1607.01363).
- [15] E. Dimastrogiovanni and R. Emami, “Correlating CMB Spectral Distortions with Temperature: what do we learn on Inflation?,” *JCAP* **1612** no. 12, (2016) 015, [arXiv:1606.04286 \[astro-ph.CO\]](https://arxiv.org/abs/1606.04286).
- [16] J. Chluba, E. Dimastrogiovanni, M. A. Amin, and M. Kamionkowski, “Evolution of CMB spectral distortion anisotropies and tests of primordial non-Gaussianity,” *Mon. Not. Roy. Astron. Soc.* **466** no. 2, (2017) 2390–2401, [arXiv:1610.08711 \[astro-ph.CO\]](https://arxiv.org/abs/1610.08711).

[17] A. Ota, “Cosmological constraints from μE cross-correlations,” *Phys. Rev.* **D94** no. 10, (2016) 103520, [arXiv:1607.00212 \[astro-ph.CO\]](https://arxiv.org/abs/1607.00212).

[18] A. Ravenni, M. Liguori, N. Bartolo, and M. Shiraishi, “Primordial non-Gaussianity with μ -type and y -type spectral distortions: exploiting Cosmic Microwave Background polarization and dealing with secondary sources,” [arXiv:1707.04759 \[astro-ph.CO\]](https://arxiv.org/abs/1707.04759).

[19] M. Remazeilles and J. Chluba, “Extracting foreground-obscured μ -distortion anisotropies to constrain primordial non-Gaussianity,” [arXiv:1802.10101 \[astro-ph.CO\]](https://arxiv.org/abs/1802.10101).

[20] N. Bartolo, S. Matarrese, and A. Riotto, “Enhancement of non-Gaussianity after inflation,” *JHEP* **04** (2004) 006, [arXiv:astro-ph/0308088 \[astro-ph\]](https://arxiv.org/abs/astro-ph/0308088).

[21] N. Bartolo, S. Matarrese, and A. Riotto, “Evolution of second - order cosmological perturbations and non-Gaussianity,” *JCAP* **0401** (2004) 003, [arXiv:astro-ph/0309692 \[astro-ph\]](https://arxiv.org/abs/astro-ph/0309692).

[22] P. Creminelli and M. Zaldarriaga, “CMB 3-point functions generated by non-linearities at recombination,” *Phys. Rev.* **D70** (2004) 083532, [arXiv:astro-ph/0405428 \[astro-ph\]](https://arxiv.org/abs/astro-ph/0405428).

[23] P. Creminelli, C. Pitrou, and F. Vernizzi, “The CMB bispectrum in the squeezed limit,” *JCAP* **1111** (2011) 025, [arXiv:1109.1822 \[astro-ph.CO\]](https://arxiv.org/abs/1109.1822).

[24] N. Bartolo, S. Matarrese, and A. Riotto, “Non-Gaussianity in the Cosmic Microwave Background Anisotropies at Recombination in the Squeezed limit,” *JCAP* **1202** (2012) 017, [arXiv:1109.2043 \[astro-ph.CO\]](https://arxiv.org/abs/1109.2043).

[25] A. Lewis, “The full squeezed CMB bispectrum from inflation,” *JCAP* **1206** (2012) 023, [arXiv:1204.5018 \[astro-ph.CO\]](https://arxiv.org/abs/1204.5018).

[26] D. Jeong and F. Schmidt, “Cosmic Clocks,” *Phys. Rev.* **D89** no. 4, (2014) 043519, [arXiv:1305.1299 \[astro-ph.CO\]](https://arxiv.org/abs/1305.1299).

[27] E. Pajer, F. Schmidt, and M. Zaldarriaga, “The Observed Squeezed Limit of Cosmological Three-Point Functions,” *Phys. Rev.* **D88** no. 8, (2013) 083502, [arXiv:1305.0824 \[astro-ph.CO\]](https://arxiv.org/abs/1305.0824).

[28] M. Mirbabayi and M. Zaldarriaga, “CMB Anisotropies from a Gradient Mode,” *JCAP* **1503** no. 03, (2015) 056, [arXiv:1409.4777 \[astro-ph.CO\]](https://arxiv.org/abs/1409.4777).

[29] L. Dai, E. Pajer, and F. Schmidt, “Conformal Fermi Coordinates,” *JCAP* **1511** no. 11, (2015) 043, [arXiv:1502.02011 \[gr-qc\]](https://arxiv.org/abs/1502.02011).

[30] L. Dai, E. Pajer, and F. Schmidt, “On Separate Universes,” *JCAP* **1510** no. 10, (2015) 059, [arXiv:1504.00351 \[astro-ph.CO\]](https://arxiv.org/abs/1504.00351).

[31] G. Cabass, E. Pajer, and F. Schmidt, “How Gaussian can our Universe be?,” *JCAP* **1701** no. 01, (2017) 003, [arXiv:1612.00033 \[hep-th\]](https://arxiv.org/abs/1612.00033).

[32] S. Weinberg, “Adiabatic modes in cosmology,” *Phys. Rev.* **D67** (2003) 123504, [arXiv:astro-ph/0302326 \[astro-ph\]](https://arxiv.org/abs/astro-ph/0302326).

[33] J. Chluba, “Green’s function of the cosmological thermalization problem,” *Mon. Not. Roy. Astron. Soc.* **434** (2013) 352, [arXiv:1304.6120 \[astro-ph.CO\]](https://arxiv.org/abs/1304.6120).

[34] G. Cabass, A. Melchiorri, and E. Pajer, “ μ -distortions or running: A guaranteed discovery from CMB spectrometry,” *Phys. Rev.* **D93** no. 8, (2016) 083515, [arXiv:1602.05578 \[astro-ph.CO\]](https://arxiv.org/abs/1602.05578).

[35] J. Chluba, “Which spectral distortions does Λ CDM actually predict?,” *Mon. Not. Roy. Astron. Soc.* **460** no. 1, (2016) 227–239, [arXiv:1603.02496](https://arxiv.org/abs/1603.02496) [[astro-ph.CO](#)].

[36] J. Chluba and R. A. Sunyaev, “The evolution of CMB spectral distortions in the early Universe,” *Mon. Not. Roy. Astron. Soc.* **419** (2012) 1294–1314, [arXiv:1109.6552](https://arxiv.org/abs/1109.6552) [[astro-ph.CO](#)].

[37] R. Khatri and R. A. Sunyaev, “Beyond y and μ : the shape of the CMB spectral distortions in the intermediate epoch, $1.5 \times 10^4 < z < 2 \times 10^5$,” *JCAP* **1209** (2012) 016, [arXiv:1207.6654](https://arxiv.org/abs/1207.6654) [[astro-ph.CO](#)].

[38] R. Khatri and R. A. Sunyaev, “Forecasts for CMB μ - and i -type spectral distortion constraints on the primordial power spectrum on scales $8 \text{ Mpc}^{-1} \lesssim k \lesssim 10^4 \text{ Mpc}^{-1}$ with the future Pixie-like experiments,” *JCAP* **1306** (2013) 026, [arXiv:1303.7212](https://arxiv.org/abs/1303.7212) [[astro-ph.CO](#)].

[39] S. Weinberg, “Entropy generation and the survival of protogalaxies in an expanding universe,” *Astrophys. J.* **168** (1971) 175.

[40] S. Weinberg, *Cosmology*. Oxford Univ. Pr., 2008.
<http://www.oup.com/uk/catalogue/?ci=9780198526827>.

[41] S. Dodelson, *Modern Cosmology*. Academic Press, Amsterdam, 2003.
<http://www.slac.stanford.edu/spires/find/books/www?cl=QB981:D62:2003>.

[42] V. Desjacques, D. Jeong, and F. Schmidt, “Large-Scale Galaxy Bias,” [arXiv:1611.09787](https://arxiv.org/abs/1611.09787) [[astro-ph.CO](#)].

[43] T. Baldauf, U. Seljak, L. Senatore, and M. Zaldarriaga, “Galaxy Bias and non-Linear Structure Formation in General Relativity,” *JCAP* **1110** (2011) 031, [arXiv:1106.5507](https://arxiv.org/abs/1106.5507) [[astro-ph.CO](#)].

[44] P. Creminelli and M. Zaldarriaga, “Single field consistency relation for the 3-point function,” *JCAP* **0410** (2004) 006, [arXiv:astro-ph/0407059](https://arxiv.org/abs/astro-ph/0407059) [[astro-ph](#)].

[45] P. Creminelli, J. Noreña, and M. Simonović, “Conformal consistency relations for single-field inflation,” *JCAP* **1207** (2012) 052, [arXiv:1203.4595](https://arxiv.org/abs/1203.4595) [[hep-th](#)].

[46] K. Hinterbichler, L. Hui, and J. Khoury, “Conformal Symmetries of Adiabatic Modes in Cosmology,” *JCAP* **1208** (2012) 017, [arXiv:1203.6351](https://arxiv.org/abs/1203.6351) [[hep-th](#)].

[47] P. Creminelli, J. Noreña, M. Simonović, and F. Vernizzi, “Single-Field Consistency Relations of Large Scale Structure,” *JCAP* **1312** (2013) 025, [arXiv:1309.3557](https://arxiv.org/abs/1309.3557) [[astro-ph.CO](#)].

[48] A. Lewis, A. Challinor, and A. Lasenby, “Efficient computation of CMB anisotropies in closed FRW models,” *Astrophys. J.* **538** (2000) 473–476, [arXiv:astro-ph/9911177](https://arxiv.org/abs/astro-ph/9911177) [[astro-ph](#)].

[49] A. Ota, “CMB spectral distortions as solutions to the Boltzmann equations,” *JCAP* **1701** no. 01, (2017) 037, [arXiv:1611.08058](https://arxiv.org/abs/1611.08058) [[astro-ph.CO](#)].

[50] C. W. Misner, K. S. Thorne, and J. A. Wheeler, *Gravitation*. W. H. Freeman, San Francisco, 1973.

[51] L. Senatore, S. Tassev, and M. Zaldarriaga, “Cosmological Perturbations at Second Order and Recombination Perturbed,” *JCAP* **0908** (2009) 031, [arXiv:0812.3652](https://arxiv.org/abs/0812.3652) [[astro-ph](#)].